

**Analog and Mixed-Signal Products**

# **Analog Applications Journal**

**Fourth Quarter, 2002**



### IMPORTANT NOTICE

Texas Instruments Incorporated and its subsidiaries (TI) reserve the right to make corrections, modifications, enhancements, improvements, and other changes to its products and services at any time and to discontinue any product or service without notice. Customers should obtain the latest relevant information before placing orders and should verify that such information is current and complete. All products are sold subject to TI's terms and conditions of sale supplied at the time of order acknowledgment.

TI warrants performance of its hardware products to the specifications applicable at the time of sale in accordance with TI's standard warranty. Testing and other quality control techniques are used to the extent TI deems necessary to support this warranty. Except where mandated by government requirements, testing of all parameters of each product is not necessarily performed.

TI assumes no liability for applications assistance or customer product design. Customers are responsible for their products and applications using TI components. To minimize the risks associated with customer products and applications, customers should provide adequate design and operating safeguards.

TI does not warrant or represent that any license, either express or implied, is granted under any TI patent right, copyright, mask work right, or other TI intellectual property right relating to any combination, machine, or process in which TI products or services are used. Information published by TI regarding third-party products or services does not constitute a license from TI to use such products or services or a warranty or endorsement thereof. Use of such information may require a license from a third party under the patents or other intellectual property of the third party, or a license from TI under the patents or other intellectual property of TI.

Reproduction of information in TI data books or data sheets is permissible only if reproduction is without alteration and is accompanied by all associated warranties, conditions, limitations, and notices. Reproduction of this information with alteration is an unfair and deceptive business practice. TI is not responsible or liable for such altered documentation.

Resale of TI products or services with statements different from or beyond the parameters stated by TI for that product or service voids all express and any implied warranties for the associated TI product or service and is an unfair and deceptive business practice. TI is not responsible or liable for any such statements.

Mailing Address:

Texas Instruments  
Post Office Box 655303  
Dallas, Texas 75265

Copyright © 2002, Texas Instruments Incorporated

# Contents

<b>Introduction</b> .....	4
<b>Data Acquisition</b>	
Interfacing op amps and analog-to-digital converters .....	5
This article summarizes the information needed to construct an op amp interface between an input source and an analog-to-digital converter.	
<b>Power Management</b>	
Using the UCC3580-1 controller for highly efficient 3.3-V/100-W isolated supply design .....	8
This article presents a design idea using the UCC3580 to generate an isolated 3.3-V, 30-A output from a 48-V input. An overview of the circuit operation is included with typical waveforms. The design is also compared to power modules with similar power specifications.	
Power conservation options with dynamic voltage scaling in portable DSP designs .....	12
Included in this article are two generic methods of implementing dynamic voltage scaling (DVS) along with the advantages and disadvantages of each method. The TPS62200 300-mA synchronous buck converter is used as an example, but the same solutions apply to most dc/dc converters.	
Understanding piezoelectric transformers in CCFL backlight applications .....	18
PZTs have higher efficiency, smaller size, lower electromagnetic noise, and higher available strike voltage than magnetic transformers. This article provides an overview of piezoelectric characteristics and how they relate to driving CCFL lamps.	
<b>Amplifiers: Op Amps</b>	
Active output impedance for ADSL line drivers .....	24
Active termination in ADSL systems can provide a considerable reduction in power dissipation. This article describes in-depth the trade-offs involved in using active impedance in Class-AB and Class-G amplifiers.	
<b>Index of Articles</b> .....	32
<b>TI Worldwide Technical Support</b> .....	35

To view past issues of the  
*Analog Applications Journal*, visit the Web site  
[www.ti.com/sc/analogapps](http://www.ti.com/sc/analogapps)

# Introduction

*Analog Applications Journal* is a collection of analog application articles designed to give readers a basic understanding of TI products and to provide simple but practical examples for typical applications. Written not only for design engineers but also for engineering managers, technicians, system designers and marketing and sales personnel, the book emphasizes general application concepts over lengthy mathematical analyses.

These applications are not intended as “how-to” instructions for specific circuits but as examples of how devices could be used to solve specific design requirements. Readers will find tutorial information as well as practical engineering solutions on components from the following categories:

- Data Acquisition
- Power Management
- Amplifiers: Op Amps

Where applicable, readers will also find software routines and program structures. Finally, *Analog Applications Journal* includes helpful hints and rules of thumb to guide readers in preparing for their design.

# Interfacing op amps and analog-to-digital converters

By **Bruce Carter** (Email: r-carter5@ti.com)

*Advanced Linear Products, Op Amp Applications*

## Introduction

One of the most common questions asked of the TI High-Speed Amplifiers Applications team is what op amp to use with a given analog-to-digital converter (ADC). The ADC is often from a competitor. Answering this question is a challenging task—and there is no absolute answer, only a list of gray areas and trade-offs.

It would be handy to have a table with ADCs on one side and recommended op amps on the other. But this table will never exist; there are too many variables in system design that affect op amp selection. This article does not contain answers, but questions. The questions will help the designer organize his thoughts and define exactly what the op amp needs to do. He should be prepared to answer these questions before committing to a design.

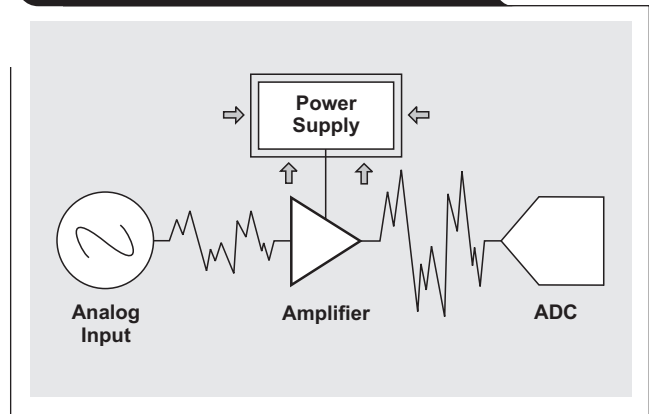
The list of questions may look daunting at first, but it is divided into sections that break up the system into component parts: system, power supply, input signal, ADC, operational amplifier, and other considerations. The completion of each section is a piece of the puzzle, and by the end of the process the designer should have weeded out op amps that are unsuitable for the job.

## System information

The overall characteristics of the system often yield valuable information. A clear understanding of the product and its function is imperative to design success.

- Exactly what is the end equipment and its application? Different systems have different requirements. For example, key concerns in a video system are completely different from those in a wireless communication system.
- In general terms, what is the function of this signal-acquisition chain in the system? Where does the input signal come from and what happens to it once it is digitized?
- How many signal-acquisition chains are used in the product? Channel density can influence system design in numerous ways, including space constraints, thermal requirements, and amplifier channel density per package.
- Will this signal chain be duplicated in other products? Is flexibility an advantage, or can the design be narrowly focused on the task at hand?
- Is the design forced to adhere to a particular standard?
- In what temperature conditions will the system operate (for example,  $-40^{\circ}\text{C}$  to  $+85^{\circ}\text{C}$ ,  $0^{\circ}\text{C}$  to  $+70^{\circ}\text{C}$ , or  $+45^{\circ}\text{C}$  to  $+55^{\circ}\text{C}$ )?
- Does the system have forced air flow from a fan to help with thermal dissipation?
- Is automatic gain control (AGC) functionality required? If so, is it digital or analog control? What is the gain range, etc.?
- Is a current solution unsatisfactory in some way? Why is the current solution unsatisfactory?

**Figure 1. Focusing on power supply characteristics**



## Power supply information

Power supply rails can quickly rule out amplifier solutions. This is similar to clothing shopping—the style may be desirable; but if the size doesn't fit, the style is useless. So a wise shopper finds the options in the size first, before becoming attached to a style. Similarly, an op amp with fantastic specifications at  $\pm 15\text{ V}$  may not operate at all from a  $+3.3\text{-V}$  power supply. Power supply information is collected first, because it will simply and unequivocally narrow choices. See Figure 1.

- What is the power budget for the overall system? Is power a concern, or is performance the ultimate goal?
- What power supply voltages are available in the design?
- Is there a preferred power supply voltage for the amplifier circuitry?
- Can an additional supply voltage be added if performance could be improved? Often, the best amplifier performance can be obtained with split supplies.
- Is a precision reference available in the system? In single-supply systems, it is important to supply a virtual ground to the op amp circuitry. If the system contains a reference, it would be advantageous to utilize it.
- Are there any special characteristics of the power supply? For example, is the power supply a switching power supply? Although op amps usually have excellent power supply rejection, it could be a concern in a high-resolution system. Any widely varying loads could also affect the op amp supply voltage.

## Input signal characteristics

Understanding the input source is key to proper design of the interface circuitry between the source and the ADC (see Figure 2).

- What is used for the signal source to the amplifier block in front of the ADC? Is it another amplifier, a sensor, etc.?
- Describe the input signal. For example, is it continuous or discontinuous (i.e., pulsed)? The signal might be a QAM signal, an NTSC signal, a non-standard continuous wave signal, a random analog signal, etc.
- Are there any unusual characteristics of the signal source? Some sources have characteristics that will affect the performance of the amplifier circuit. For example, photodiodes have an associated capacitance, and the value of this capacitance plays an important role in how the associated amplifier circuit is designed.
- What is the output amplitude range of the source?
- Does the source produce a voltage or a current output?
- Is the signal source output single-ended or differential?
- What is the output impedance of the signal source?
- Is the input signal dc-referenced? If so, to what dc voltage is it referenced?
- What are the frequency characteristics of the input signal? For example, the signal might have a 10-MHz bandwidth centered around 25 MHz, or it might be a signal with frequency content from dc up to 20 MHz. If low frequency isn't important, this opens the possibility of ac coupling the input signal.
- What level of rejection is required out-of-band? Some applications have very strict requirements for out-of-band rejection, while others are less strict. The filter interface between the amplifier network and the ADC is dictated by this sort of information.
- Is there a known interfering frequency (system clock, sample clock, etc.) that must be filtered out? Are other large signals expected outside of the band of interest? A simple low-pass filter often may not have sufficient rejection of a particular interfering signal, forcing additional circuitry to produce a high Q notch filter.
- Is there a requirement for gain or phase flatness or error? This is a concern in video systems.
- Is there a matching requirement on the input impedance of the amplifier circuit? Some circuits require that the load be matched to a particular value for optimal performance (e.g., 50  $\Omega$ ).

## ADC characteristics

Once the power supply and input signal have been defined, it is time to focus on the device that the op amp will drive—the ADC (see Figure 3).

- Has the ADC been selected, or can it be changed to enhance performance?
- What is the desired sampling rate? Designers often assume that a data converter is going to be used at its maximum level of performance, but this typically isn't the case. For example, an 80-megasample-per-second (MSPS) converter might be given a sampling frequency of 60 MSPS.

Figure 2. Focusing on the input signal

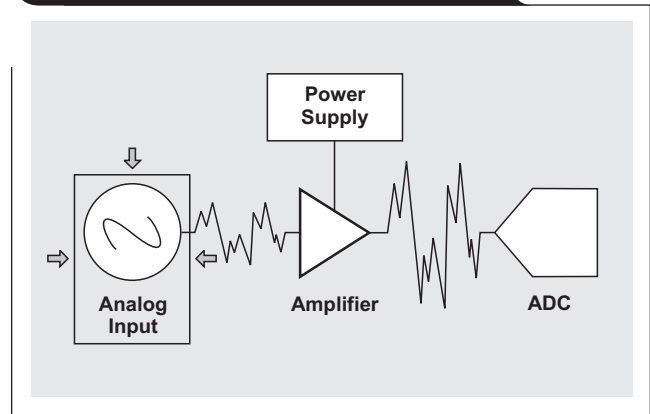
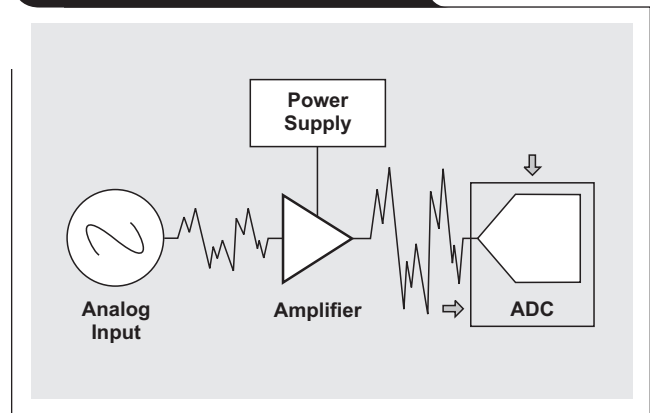


Figure 3. Focusing on the ADC



- What is the desired resolution and effective number of bits? A 14-bit converter won't effectively yield 14 bits. The true resolution will probably be closer to 12 or 13.
- What is the full-scale input range of the data converter? Some data converters permit the input to be configured for different ranges.
- Will the data converter be used with single-ended or differential inputs? Typically, most high-performance data converters have differential inputs and require their use for optimal performance.
- Are there any other options on the data converter that could be an advantage? Data converters have lots of options that vary from part to part.
- Are there any compensation requirements for the input of the data converter? Normally, a small RC filter is required at the input of the data converter to compensate for its capacitive input. These components are usually specified in the converter data sheet and should be included as part of the interface. Otherwise, the op amp interface circuit may exhibit instability.

## Operational amplifier characteristics

Although this article is intended to aid in the selection of the correct operational amplifier, it is possible that the nature of the system already defines some characteristics. See Figure 4.

- Has the operational amplifier already been selected, or can it be changed to improve system performance?
- Are there specific requirements for the package of the amplifiers? For example, must it be an 8-pin SOIC, or as small as possible, etc.?
- Does the cost of the operational amplifier interface or the physical size of the interface circuitry dictate that as few operational amplifiers as possible be used? Or would it be an advantage for the circuitry to be easily modified in the future, using more operational amplifiers for the flexibility?

## Other pertinent considerations

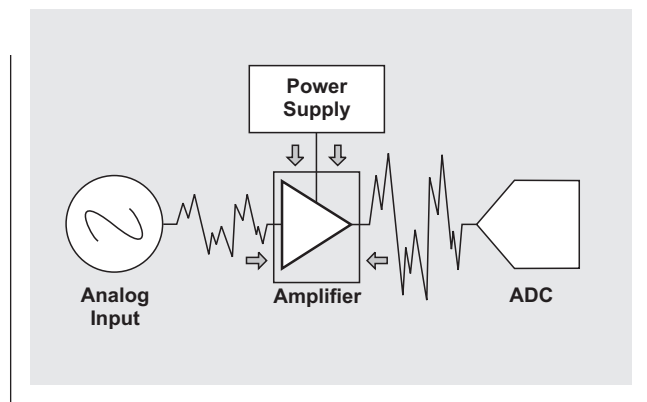
This is the point at which the definition of the system should be complete. The wise designer, however, should take a step back. He should be asking, "Are there any other questions I should have asked? If questions were not asked, why not?"

The biggest consideration of all may be cost. This single concern has the potential of forcing a lot of good design work to be thrown on the trash heap. Yet a wise designer seldom goes wrong if he keeps the cost and number of components in mind when creating his design. Whether a million systems are produced, or only one, every manager will be pleased if the cost can be reduced without compromising system performance.

## Conclusion

The design of a data acquisition system is a complex and time-consuming task. There are no universal solutions, nor are there any reliable lists of which op amp is matched to which ADC. There are a great number of factors affecting performance, and each design should be approached as if it were a custom design for which no precedent exists.

Figure 4. Focusing on the operational amplifiers



The designer must first answer the questions presented earlier to gain a good understanding of the true nature of his system and the scope of his design task. The next step is to visit [amplifier.ti.com](http://amplifier.ti.com) and look in the op amp selection guides for op amps that fit the application. As a general rule, the op amp should be much better than the data converter to which it is interfaced; otherwise, the designer is wasting money on the data converter.

In addition to the "Related Web sites" below, TI has a semiconductor technical support knowledge base to assist designers in finding products and services related to their technical questions. The direct link to this knowledge base is [support.ti.com/sc/knowledgebase](http://support.ti.com/sc/knowledgebase)

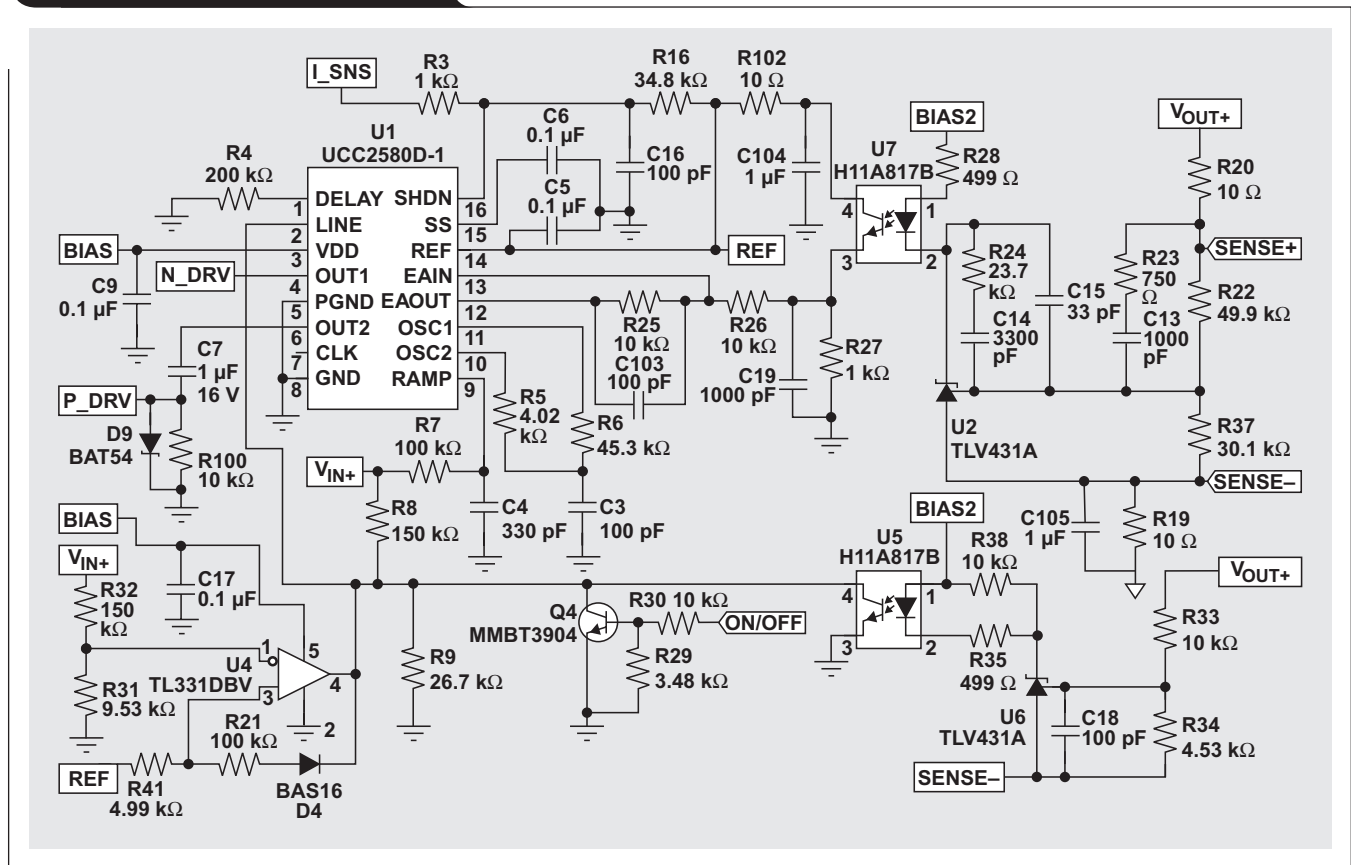
For more general support information, visit [support.ti.com](http://support.ti.com)

## Related Web sites

[analog.ti.com](http://analog.ti.com)  
[amplifier.ti.com](http://amplifier.ti.com)  
[dataconverter.ti.com](http://dataconverter.ti.com)



Figure 2. Control stage schematic



$V_{IN}$ . This allows softer turn-on and reduces switching losses in Q1 (see Figure 4).

The secondary power stage consists of the synchronous rectifiers (Q5, Q6, Q8, and Q9) and the output filter (L1, C1, C11, C12, and C102). When Q1 is on, the voltage on the secondary of T1 ensures that both Q8 and Q9 are on, while Q5 and Q6 are off. During this time, a voltage equal to the input voltage divided by the turns ratio of the

transformer is applied across the gate-to-source of Q8 and Q9, and also across the drain-to-source of Q5 and Q6. Also during this time, the gate-to-source voltage of Q5 and Q6 is essentially 0 V and is equal to the inductor current times the  $r_{ds(on)}$  of Q8 and Q9.

When Q2 is off, the voltage on the secondary of T1 reverses, and ensures that both Q5 and Q6 are on, while Q8 and Q9 are off. During this time, the magnitude of the

Figure 3. Power MOSFET drain waveforms

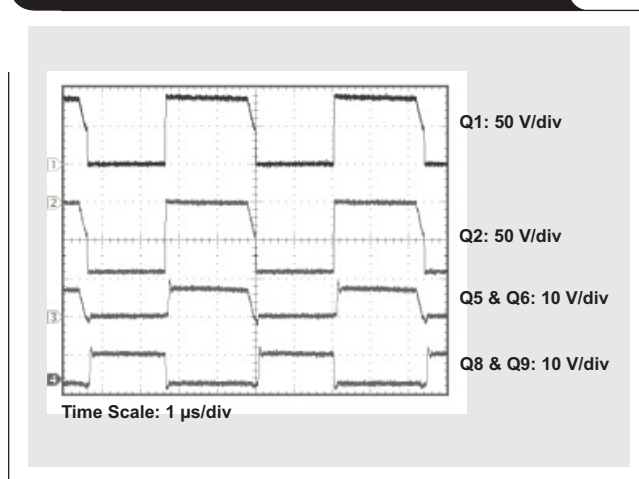
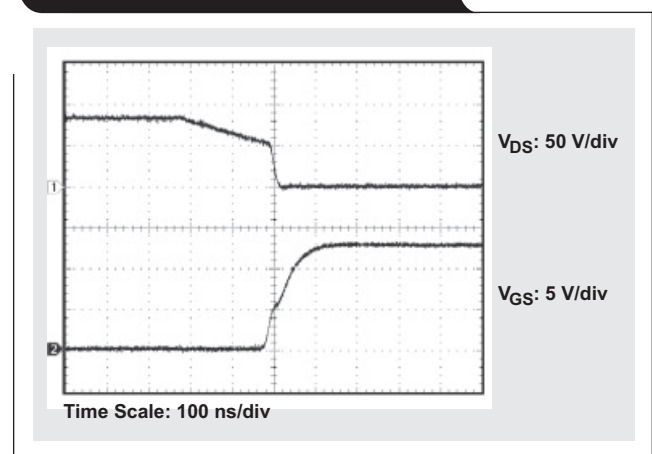


Figure 4. Turn-on of primary-side n-channel MOSFET



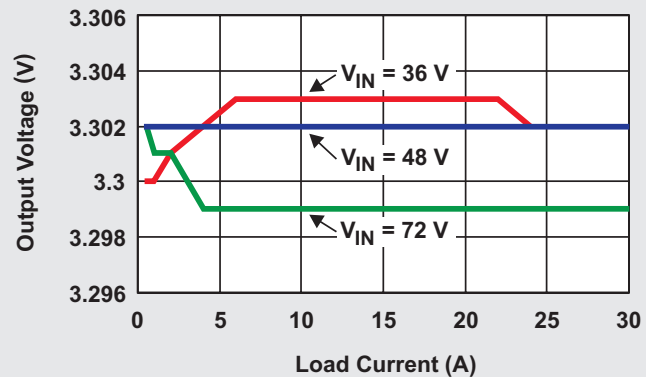
transformer secondary voltage is equal to the clamp capacitor voltage minus the input voltage, divided by the transformer turns ratio. The peak clamp capacitor voltage will determine the maximum voltage stress across the gate-to-source of Q5 and Q6, and also across the drain-to-source of Q8 and Q9. During this time, the gate-to-source voltage of Q8 and Q9 is essentially 0 V and is equal to the inductor current times the  $r_{ds(on)}$  of Q5 and Q6.

Two bias voltages are used in this active-clamp design, one for the primary side and one for the secondary side. The circuit composed of C8, D2, D3, L1, Q3, and R12 produces the primary-side bias. D2, R12, and Q3 form a linear regulator, which is functional only during startup, or during a fault condition. L1 contains an auxiliary winding that is used to produce the primary-side bias during normal operation. The main winding of L1 has 4 turns, while the auxiliary winding has 16 turns. The auxiliary winding charges C8 to a voltage equal to the output voltage times the 16:4 turns ratio of the inductor, minus the diode drop of D3.

The circuit composed of C100, C101, D100, D101, Q100, and R101 produces the secondary-side bias. This bias is required to drive the feedback optocoupler (U7) and the TLV431 (U2). D100 and C100 peak detect the transformer secondary voltage. R101, D101, and Q100 form a linear regulator. The linear regulator is necessary to ensure that the bias voltage is independent of the input voltage. Without the linear regulator circuit, a second feedback loop is introduced into the compensation circuit, which complicates the compensation design.

Breaking the feedback path with R19 and R20 provides remote sensing. By connecting the remote sense terminals directly to the desired regulation point, the converter compensates for any voltage drops between the output of the supply and the load. The remote sense terminals must always be connected to the converter output and output return. If remote sensing is not required, R19 and R20 may be shorted, in which case regulation will be provided directly at the converter output filter.

Figure 5. Line and load regulation

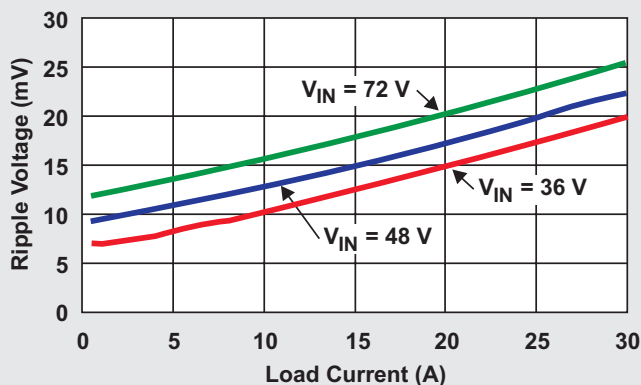


The feedback network is typical of most isolated forward converters. The TLV431 (U2) incorporates a voltage reference and transconductance error amplifier into one package. Providing type III compensation around U2 compensates the voltage-mode converter. The current transfer ratio of U7 and the values of R27 and R28 determine the gain of the optocoupler circuit. The error amplifier of the UCC3580-1 is used in an inverting configuration, with a gain of 1 V/V.

The shutdown pin of the UCC3580-1 provides overcurrent protection. The current is sensed at the source of Q1 by resistors R2 and R103. Resistor R16 lowers the shutdown threshold voltage, which improves the converter's efficiency by decreasing the required resistance of R2 and R103.

The UCC3580-1 and resistors R8 and R9 control the input undervoltage protection. The comparator circuit of U4 controls input overvoltage protection. Both input overvoltage and input undervoltage circuits provide hysteresis. The circuit of U5 and U6 provides output overvoltage protection. When the input to U6 exceeds the TLV431 reference voltage, the converter shuts down until the overvoltage condition is gone, at which point a normal soft-start cycle is initiated.

Figure 6. Output ripple voltage



## Performance

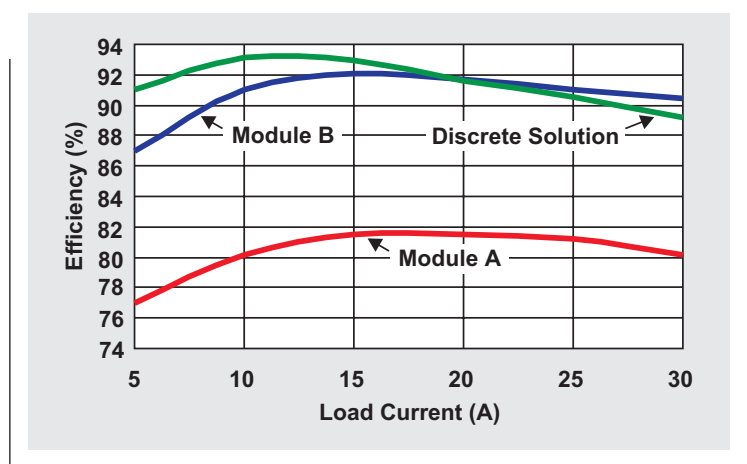
The circuit operates from input voltages between 36 and 75 V and at load currents of up to 30 A. The output voltage typically varies by only 4 mV (0.1%) over the entire line and load range (see Figure 5). Most power modules with similar power requirements list line and load regulations below 0.2%. The output ripple voltage of this design is kept below 26 mV (0.8%) over line and load, as shown in Figure 6. Power modules offer similar ripple performance.

Figure 7 compares the efficiency of this design to the efficiency of modules from two leading module manufacturers. The data are given for a 48-V input and 25°C ambient temperature. Module A is typical of the majority of 3.3-V, half-brick, 100-W modules. Module B is an example of one of the few modules that list efficiency at greater than 90%. The discrete design competes very well with even the most efficient power-supply modules. The efficiency peaks at 93% at around 12 A and drops to 89% at full-rated load.

The efficiency, package, and thermal environment all conspire to limit the maximum load current for an application. While power modules may be rated for 30 A of load current, the current may actually be limited to a fraction of this by the internal device junction temperatures. The same is true of the discrete design. Modules have an advantage in this arena because they often are constructed with materials that provide good heat-sinking properties. With a discrete design, however, the designer has the opportunity to lay out the circuit board to accommodate for the power dissipation of hot components. Even with an excellent layout, at these power levels, both the modules and discrete solution typically require some forced air flow to achieve the maximum rated current.

To compare the thermal performance of the discrete design to that of the power modules, the circuit was constructed on a 2-oz. copper, 4-layer PCB in a half-brick footprint (2.3" x 2.2"). The safe-operating-area (SOA) curves of the modules and the discrete design are shown in Figure 8 for a 48-V input and 300 linear feet per minute (lfm) of air flow. The good heat sinking and high efficiency of Module B allow it to operate at higher currents than both Module A and the discrete design. However, even the good heat sinking of Module A cannot make up for its low efficiency. Incorporating the discrete design into a larger PCB allows more copper to be tied to the hot components (the power MOSFETs) to provide a wider SOA.

Figure 7. Comparison of typical efficiencies



## Conclusion

The decision whether to build a discrete power supply or to buy premanufactured modules involves trade-offs involving cost, schedule, and risk. Designing a power supply based on a reference design, such as the one presented here, significantly lowers the risk associated with the discrete approach. In situations where schedule is key, modules are the logical choice. However, migrating to a discrete power supply yields significant cost savings, particularly in high-volume applications.

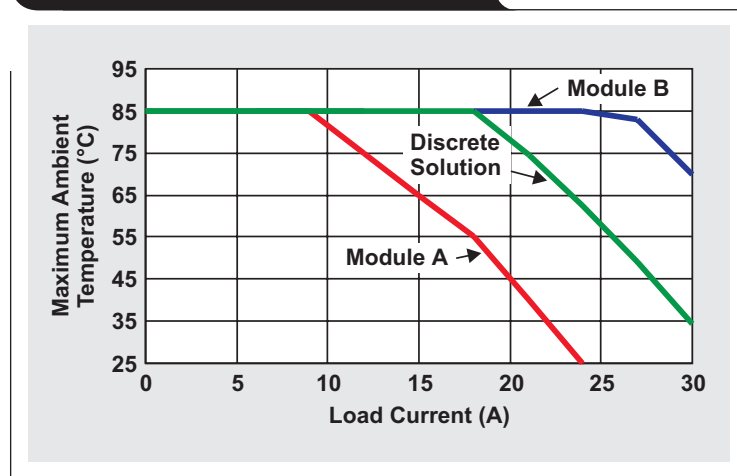
## Related Web sites

[analog.ti.com](http://analog.ti.com)

[www.ti.com/sc/device/partnumber](http://www.ti.com/sc/device/partnumber)

Replace *partnumber* with TL331, TLV431A, UCC2580-1 or UCC3580-1

Figure 8. Comparison of SOA curves



# Power conservation options with dynamic voltage scaling in portable DSP designs

By Jeff Falin (Email: j-falin1@ti.com)

*Low Power DC/DC Applications, High Performance Analog*

Extending the useful life of the battery in portable electronics with a DSP core is a challenge for portable electronics manufacturers. The relationship  $P_C \sim (V_C)^2 f$  describes the power consumption of a DSP core, where  $P_C$  is the core power consumption,  $V_C$  is the core voltage, and  $f$  is the core clock frequency.

Thus, power consumption can be reduced by lowering the internal clock frequency and/or even more by lowering the core supply voltage. Dynamic voltage scaling (DVS) is

the term used to describe methods of adjusting core supply voltage to minimize power consumption. This article explains two generic methods of implementing DVS and highlights the advantages and disadvantages of each method.

Both methods require the use of a power IC with an adjustable output voltage and an externally applied control signal ( $V_X$ ). As shown in Figures 1a and 1b, the first method uses FET switches and resistors in parallel with either the top or bottom feedback resistors to alter the feedback

**Figure 1. Methods of implementing dynamic voltage scaling**

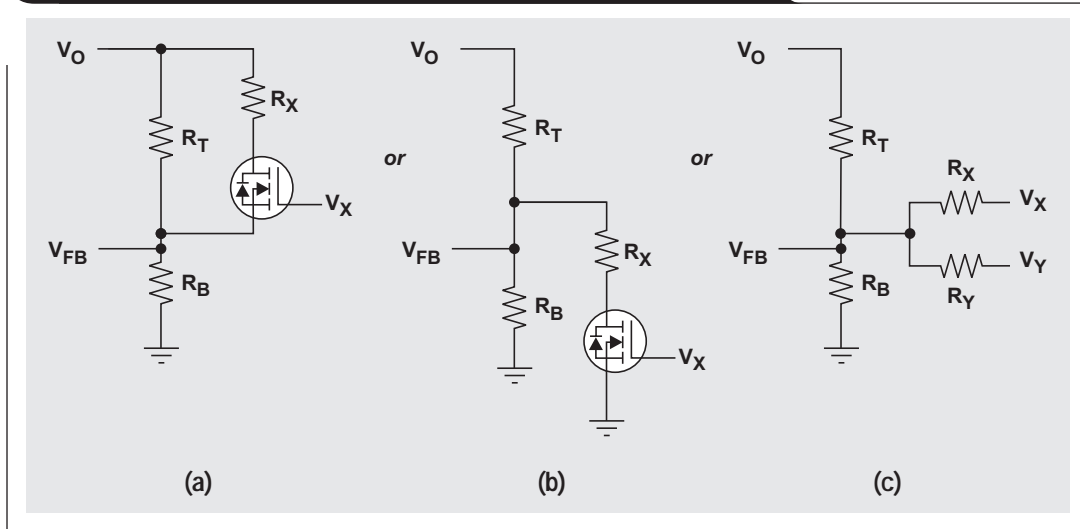
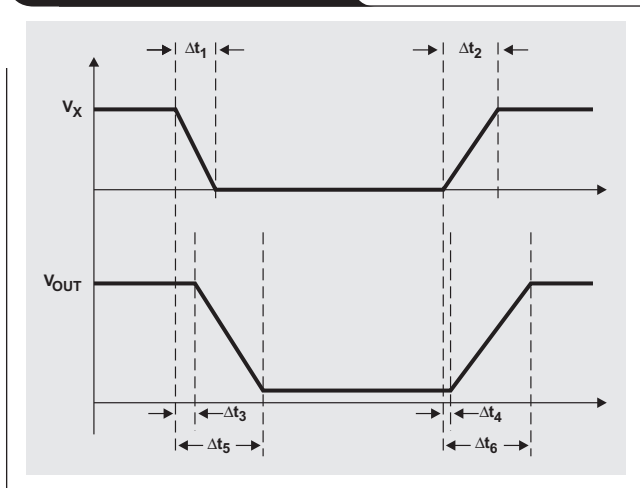


**Figure 2. Timing diagram**



network. The second method, in Figure 1c, uses the control signal or signals and an additional resistor to alter the feedback network.

Figure 2 shows the timing of the control signals and of the output voltage. Table 1 explains the different delays and their respective causes.

**Table 1. Timing delays and their causes**

	DESCRIPTION	INFLUENCING FACTORS
$\Delta t_1$	Fall time of $V_X$	Source of control signal
$\Delta t_2$	Rise time of $V_X$	
$\Delta t_3$	Response delay	Rise/fall time of $V_X$ , IC response time, feedback network settling time
$\Delta t_4$	Response delay	
$\Delta t_5$	$V_{OUT}$ fall time	Load current, output capacitance, IC response time
$\Delta t_6$	$V_{OUT}$ rise time	

Each method in Figure 1 will be examined in detail. Although most adjustable power ICs can be used to implement DVS, the author chose the TPS62200 300-mA, synchronous buck converter because it maintains high efficiency over a wide load range by switching from PFM at light loads to PWM at heavy loads.

### Switched bottom-side feedback resistor

The polarity of the control signal determines the placement of the FET switch. If a low signal triggers the step-down of the core voltage, then an NMOS FET switch and additional resistor can be placed in parallel with the bottom feedback resistor. An example application is shown in Figure 3.

Figure 4 shows an example of DVS using the circuit of Figure 3, where the input capacitance of Q2 is 110 pF. The input voltage is 3.3 V, and the output voltage switches between 1.5 V and 1.1 V with a 10-Ω load. The rise and fall times of  $V_X$  are 10 μs.

The overshoot during the transition from high to low voltage is due to the negative edge of the control signal being injected into the feedback pin, FB, by the gate-drain capacitance of the FET. Pulling FB low causes  $V_O$  to go high. Using lower-valued feedback resistors and higher-valued capacitive divider capacitors reduces the overshoot. Also, using a FET with lower input capacitance reduces the overshoot. Figure 5 shows an example of DVS using the circuit of Figure 3, where  $R_T = 200\text{ k}\Omega$ ,  $R_B = 165\text{ k}\Omega$ ,  $C_T = 100\text{ pF}$ ,  $C_B = 220\text{ pF}$ , and Q1 is a BSS123 with input capacitance of 30 pF.

If the control signal's ramp rate ( $\Delta t_1$  and  $\Delta t_2$  of Figure 1) can be slowed either at the source or by an RC filter, like the one created by  $R_F$  and  $C_F$  in Figure 3, the overshoot can be further minimized. Slowing the fall time of  $V_X$  to 150 μs removes the overshoot entirely, as shown in Figure 6.

Figure 3. Schematic with bottom resistor and high-cap FET

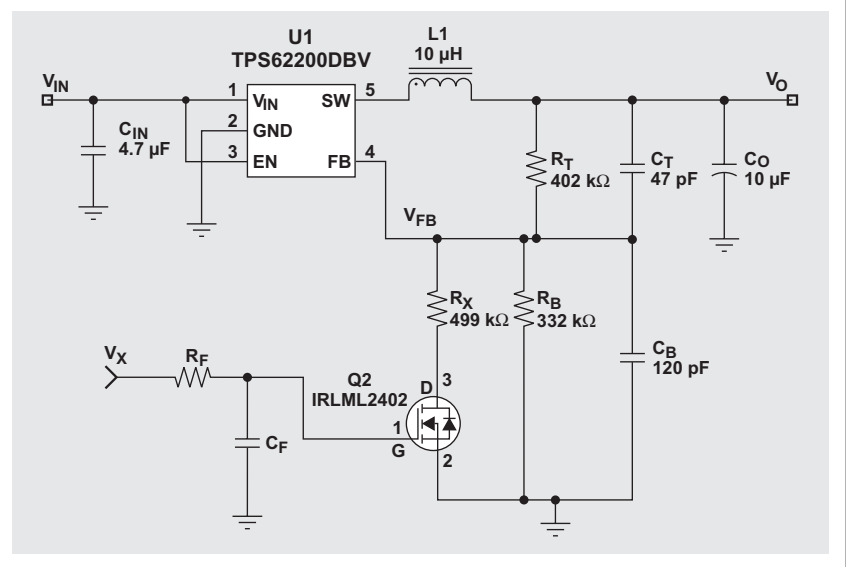


Figure 4. Bottom FET solution with overshoot

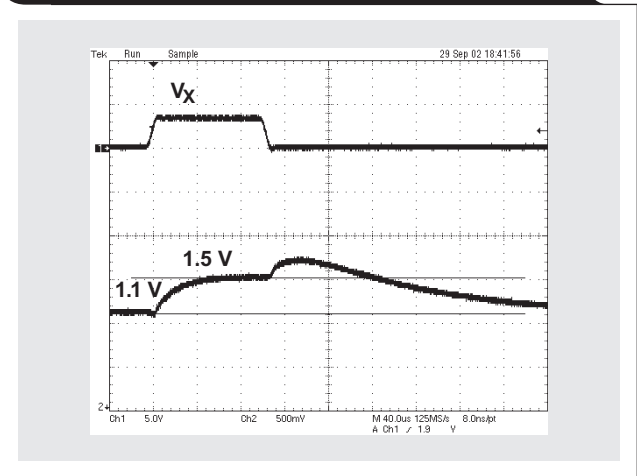


Figure 5. Bottom FET solution with reduced overshoot

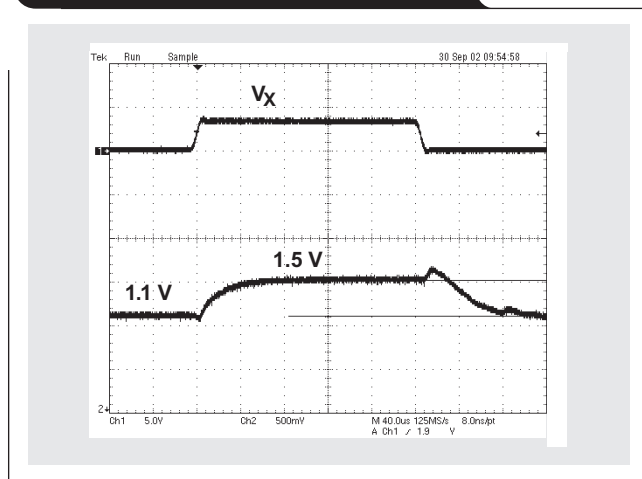
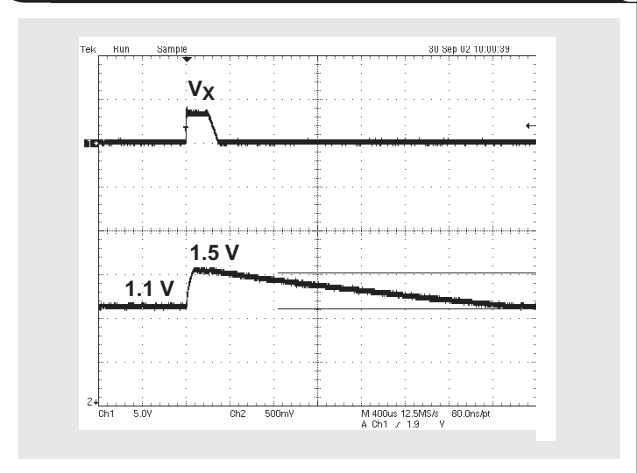
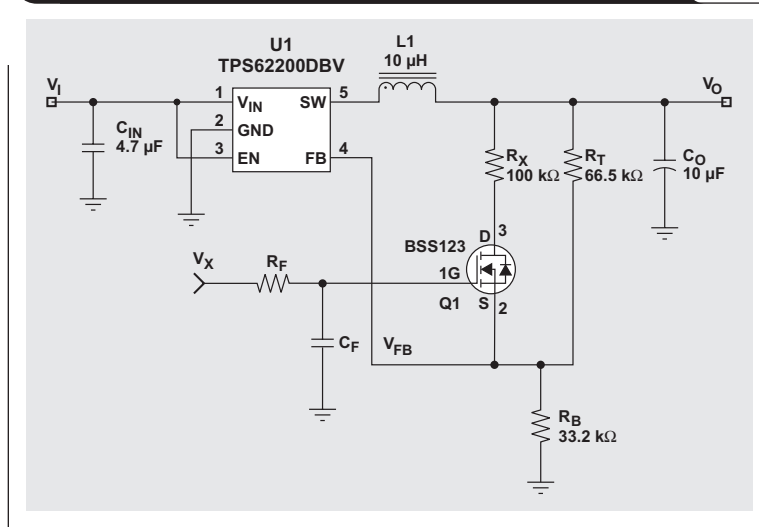


Figure 6. Bottom FET solution with no overshoot



**Figure 7. Schematic with top-side, low-cap FET and low-value feedback resistors**



**Switched top-side feedback resistor**

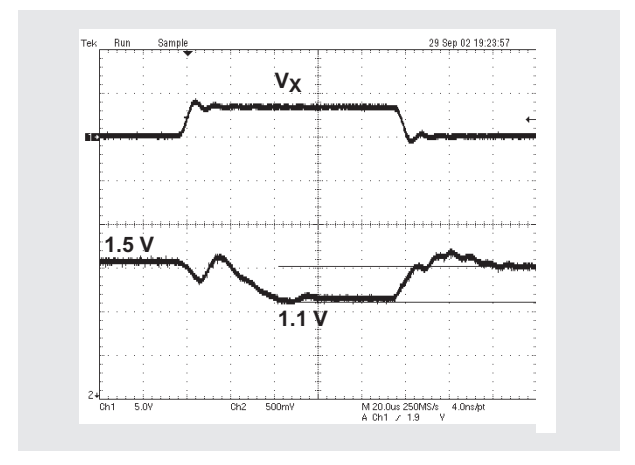
If a high control signal triggers a step-down of the output voltage, then the NMOS FET must be placed in series with the high-side feedback resistor, as shown in Figure 7. The FET must be carefully selected to ensure that (1)  $V_X$  is higher than  $V_{FB}$  by at least the FET's threshold voltage and (2) the input capacitance is low to minimize injection of  $V_X$  onto  $V_{FB}$ . Unlike the low-side FET switch in Figure 2, the high-side FET's source pin connects directly to the converter's feedback pin. Since the FET's gate-source capacitance shorts  $V_X$  to  $V_{FB}$  during its transition, the output is susceptible to overshoot and undershoot; however, lower feedback resistors reduce both.

Figure 8 shows an example of DVS using the circuit of Figure 7, with  $V_{IN} = 3.3$  V, a 10- $\Omega$  load, and control signal rise and fall times of 5  $\mu$ s.

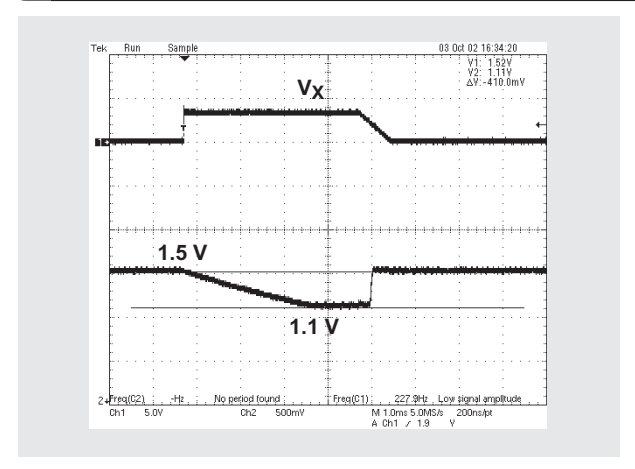
At output currents below 60 mA, the TPS62200 switches from PWM mode to PFM mode, and the observed undershoot and overshoot change. If  $V_X$ 's ramp rate ( $\Delta t_1$  and  $\Delta t_2$  of Figure 1) can be slowed either from the source or by an RC filter, like the one created by  $R_F$  and  $C_F$  in Figure 7, the overshoot is further minimized. Figure 9 shows results from using the same circuit as in Figure 7 but with a 1-k $\Omega$  load and control signal rise and fall times of 3  $\mu$ s and 500  $\mu$ s, respectively.

Although exact values for the feedback components and rise and fall times of the control signal are dependent on the specific application, the following generalizations can be made. Lower-valued feedback components reduce noise susceptibility at the feedback node and therefore reduce potential overshoot and undershoot caused by the switching transistor. However, these lower-valued feedback components consume power and reduce efficiency at light load. The rise and fall times of the control signal affect overshoot and undershoot. The optimal rise and fall times should be determined experimentally for the specific application, especially for the load current and dc/dc converter operating mode.

**Figure 8. Top-side FET solution with overshoot**



**Figure 9. Top-side FET solution at low current and reduced overshoot**



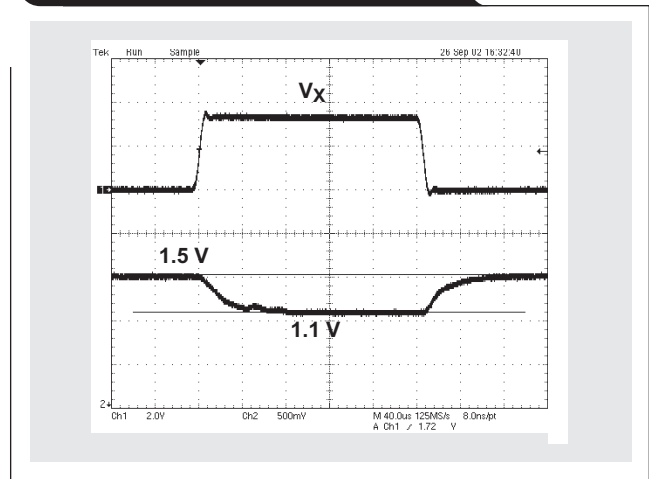
## Two voltages with one additional resistor

A simpler alternative for generating multiple voltages is to use  $V_X$  to inject current into the feedback network through an additional resistor, thereby changing the output voltage. Figure 10 shows the circuit in Figure 11 transitioning between  $V_{O1} = 1.5\text{ V}$  and  $V_{O2} = 1.1\text{ V}$ , with only one additional resistor,  $R_X$ .

For the following discussion, refer to Equations 1–4 at the bottom of this page. Equations 1 and 2 were written by summing the currents at the feedback node,  $V_{FB}$ . Simultaneously solving Equations 1 and 2, then substituting back and solving for  $R_B$ , yields Equations 3 and 4. These equations show how to compute the values of the injection resistor,  $R_X$ , and bottom feedback resistor,  $R_B$ , in Figure 11, given  $R_T = 402\text{ k}\Omega$ ,  $V_{O1} = 1.5\text{ V}$ ,  $V_{O2} = 1.1\text{ V}$ ,  $V_{X\_HI} = 3.3\text{ V}$ ,  $V_{X\_LO} = 0\text{ V}$ , and  $V_{FB} = 0.5\text{ V}$ .

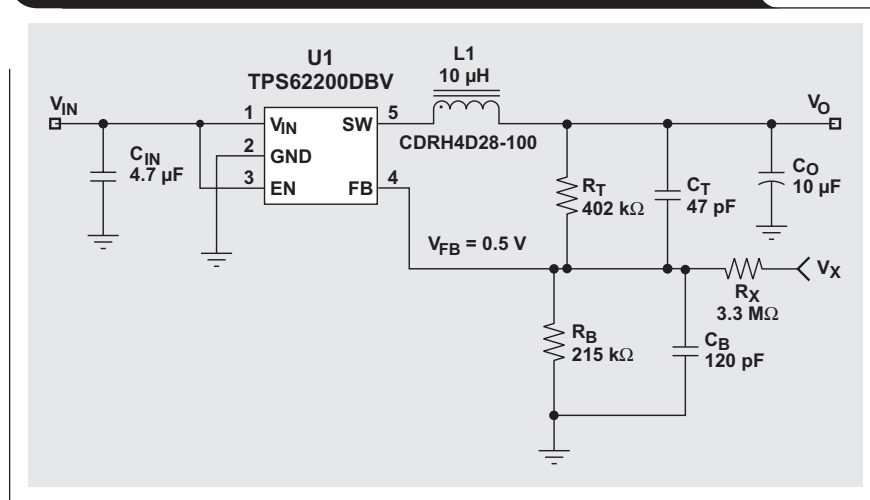
Pulsing  $V_X$  with varying duty cycles varies its average dc level. This allows a single control voltage and one additional resistor,  $R_X$ , to generate multiple output voltages. Equations 1 and 2 can be solved to find  $R_X$  and  $R_B$  for the lowest desired output voltage and highest  $V_X$ . Then, solving Equation 4 for  $V_O$  and substituting in progressively lower values for  $V_{X\_HI}$  results in progressively higher values of  $V_O$ . Figure 12 on the next page shows such an implementation.

Figure 10. Transition between two output voltages



Choosing  $R_F$  in Figure 12 two orders of magnitude below  $R_X$  eliminates the need to include it in the computation of  $R_X$ . Choosing  $C_F$  to form a low-pass filter with  $-3\text{-dB}$  roll-off at least two orders of magnitude below the frequency of  $V_X$  makes the ripple being injected into  $V_{FB}$  negligible.

Figure 11. Schematic for switching between two voltages



$$\frac{V_{FB}}{R_B} + \frac{V_{FB} - V_{O1}}{R_T} + \frac{V_{FB} - V_{X\_LO}}{R_X} = 0 \quad (1)$$

$$\frac{V_{FB}}{R_B} + \frac{V_{FB} - V_{O2}}{R_T} + \frac{V_{FB} - V_{X\_HI}}{R_X} = 0 \quad (2)$$

$$R_B = -V_{FB} R_T \times \frac{-V_{X\_HI} + V_{X\_LO}}{(-V_{O1} + V_{O2} + V_{X\_LO} - V_{X\_HI}) \times V_{FB} - V_{X\_LO} V_{O2} + V_{X\_HI} V_{O1}} \quad (3)$$

$$R_X = R_B \times R_T \times \frac{-V_{FB} + V_{X\_HI}}{V_{FB} R_B + V_{FB} R_T - V_{O2} R_B} \quad (4)$$

### Three voltages from two additional resistors

If varying the duty cycle of  $V_X$  is not an option but additional control voltages (e.g.,  $V_Y$ ) are available, the converter can still be configured to switch between multiple voltages. In addition to the two feedback resistors,  $R_T$  and  $R_B$ , this solution requires one less resistor than the number of required output voltages. For example, if the application requires switching between three different voltages, the solution requires two injection resistors,  $R_X$  and  $R_Y$ , as shown in Figure 13.

As Table 2 shows, there are four logic states that can be derived from the two logic signals,  $V_X$  and  $V_Y$ ; however, only three logic states are used.

Table 2. Control signal vs. output voltage

	$V_X$	$V_Y$	DESIRED $V_O$ (V)	ACTUAL $V_O$ (V)
$V_{O1}$	LO	LO	1.80	1.80
$V_{O2}$	LO	HI	1.50	1.50
$V_{O3}$	HI	LO	Don't care	1.40
$V_{O4}$	HI	HI	1.10	1.10

Figure 12. Filter for switching between multiple voltages

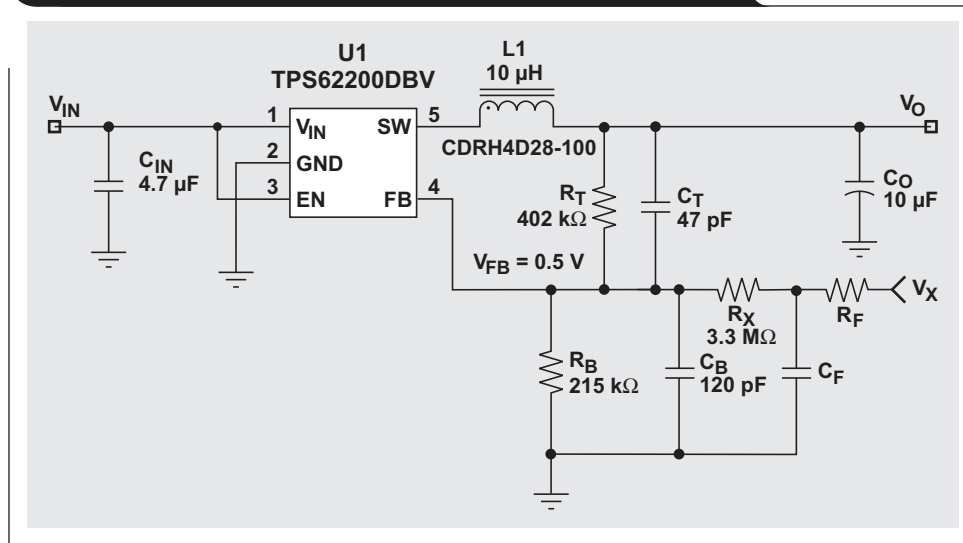
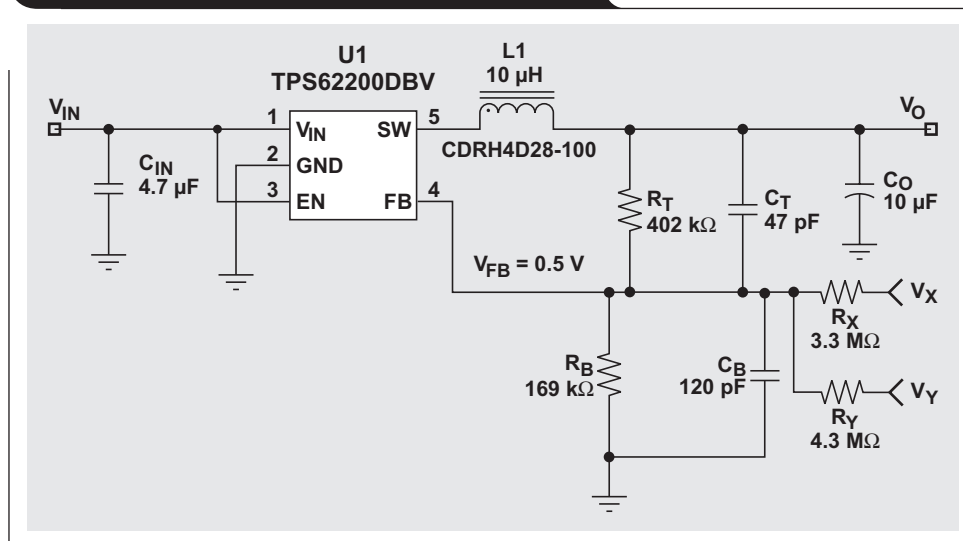


Figure 13. Switching between three voltages



Similar to the computations for Figure 11, the circuit operation of Figure 13 can be evaluated with four nodal equations (one for each logic state), which can be solved for  $R_X$ ,  $R_Y$ , and  $R_B$  in Equations 5, 6, and 7.

$$R_X = R_T \times \frac{V_{X\_LO} - V_{X\_HI}}{-V_{O2} + V_{O4}} \quad (5)$$

$$R_Y = R_T \times \frac{-V_{Y\_LO} + V_{Y\_HI}}{V_{O1} - V_{O2}} \quad (6)$$

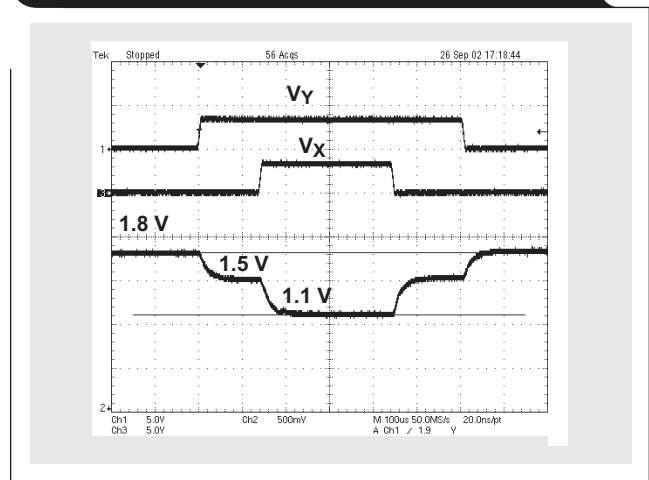
$$R_B = \left( \frac{V_{O1}/V_{FB} - 1}{R_T} - \frac{1}{R_X} - \frac{1}{R_Y} \right)^{-1} \quad (7)$$

$V_{O3}$  is not included in the equations, indicating that one of the four voltages is not independent of the others. The exact state/voltage that is not independent is determined by the method used to derive Equations 5, 6, and 7 but is one of the states during which the control signals are opposites (the second or third state in Table 2). In this case, the third state with  $V_{X\_HI}$  and  $V_{Y\_LO}$  is the dependent state and produces 1.40 V. Equations 5, 6, and 7 were used to find values for resistors  $R_X$ ,  $R_Y$ , and  $R_B$  in Figure 13, given  $R_T = 402 \text{ k}\Omega$ ,  $V_{O1} = 1.8 \text{ V}$ ,  $V_{O2} = 1.5 \text{ V}$ ,  $V_{O4} = 1.1 \text{ V}$ ,  $V_{X\_HI} = 3.3 \text{ V}$ ,  $V_{X\_LO} = 0 \text{ V}$ ,  $V_{Y\_HI} = 3.3 \text{ V}$ ,  $V_{Y\_LO} = 0 \text{ V}$ , and  $V_{FB} = 0.5 \text{ V}$ . Figure 14 shows the transition between the levels when  $V_{IN} = 3.3 \text{ V}$  and  $R_{LOAD} = 10 \Omega$ , using the circuit in Figure 13.

When injection resistors are used instead of FET switches, the transitions between voltages are much smoother.

Dynamic voltage scaling is a means of conserving power and therefore of extending battery life in portable electronics. There are two basic methods of implementing

Figure 14. Transition between three voltages



DVS using any adjustable power IC and an external control signal. If the control signal has a poor tolerance or can drive only capacitive loads, then the first method, consisting of FET switches in series with additional feedback resistors, is recommended. If the control signal has an acceptable tolerance and can drive a small resistive load, then the second method, using the control signal to inject current into the feedback network, is a simpler option and offers smoother transitions between voltages.

#### Related Web sites

[analog.ti.com](http://analog.ti.com)

[www.ti.com/sc/device/TPS62200](http://www.ti.com/sc/device/TPS62200)

# Understanding piezoelectric transformers in CCFL backlight applications

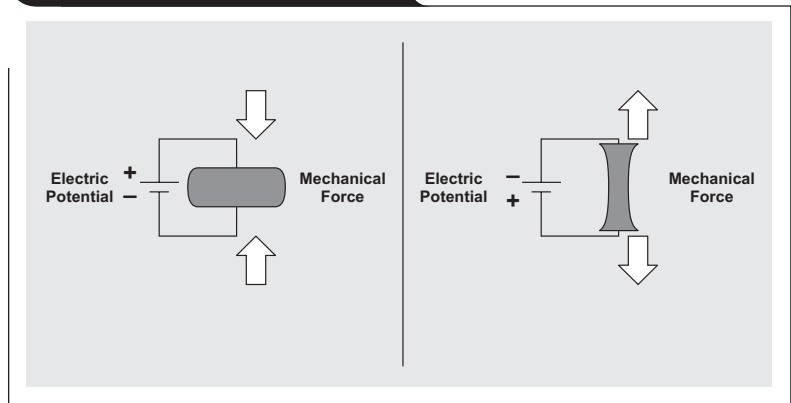
By Michael Day (Email: m-day@ti.com), Applications Manager, Portable Power Products, and Bang S. Lee (Email: banglee@ti.com), Application Specialist, Power Management

Market forces are reducing both the size and energy consumption requirements of portable devices such as PDAs, Internet appliances, and subnotebook computers. Low-profile cold cathode fluorescent lamp (CCFL) backlight solutions are commonly used in these applications. Traditional topologies have used magnetic transformers to generate the high strike and operating voltages required by CCFL lamps. The latest developments in ceramic piezoelectric transformers (PZTs) make them ideal candidates for low-profile backlight applications. PZTs have higher efficiency, smaller size, lower electromagnetic noise, and higher available strike voltage than magnetic transformers. They are also nonflammable and require only easy-to-generate sinusoidal drive voltages. Ceramic PZT operation is fundamentally different from magnetic transformer operation. A successful design requires an understanding of piezoelectric characteristics and how they relate to driving CCFL lamps.

## PZT theory

Magnetic transformers transfer energy from primary to secondary by coupling two circuit windings together through a magnetic flux path. In contrast, PZTs transfer energy from primary to secondary through the use of mechanical force. C.A. Rosen first proposed PZTs in 1956.<sup>1</sup> The basic principle of piezoelectric operation is shown in Figure 1. When an electrical potential is applied to a piezoelectric material, the electrical energy is converted to mechanical force. This is referred to as the “reverse piezoelectric effect.” When a mechanical force is applied to a piezoelectric material, the material converts the

Figure 1. Piezoelectric effect



mechanical force to electrical energy. This conversion is referred to as the “direct piezoelectric effect.”

Each manufacturer has a unique, and usually proprietary, “recipe” of materials and structural layering that determines its PZT’s operating characteristics. Common materials used to make PZTs include lead zirconate and lead titanate. A PZT may be single-layer or multilayer. Single-layer PZTs are inexpensive due to easier manufacturing processes but have relatively low voltage gains (typically 5 to 10). Multilayered PZT designs are more expensive due to the manufacturing process but have higher voltage gains (20 to 70). Multilayer PZTs are almost always used in CCFL applications because the higher gain eliminates the need for a step-up transformer and allows the CCFL to be driven with conventional off-the-shelf inductors.

Figure 2 shows a typical multilayer PZT with “longitudinal-mode” geometry. The primary has multiple layers of ceramic material with electrodes on the top and bottom. An ac voltage applied to the primary electrodes generates a mechanical force that causes the material to resonate. When the material is compressed in the vertical direction, it is expanded in the horizontal direction, and its length is increased. When it is expanded in the vertical direction, it is compressed in the horizontal direction, and its length decreases. The horizontal, or longitudinal, displacement of the primary is mechanically coupled into the secondary, which causes the secondary to vibrate. The mechanical energy in the secondary is then converted to electrical energy, which is transferred to the circuit through the secondary electrode.

Figure 2. Typical longitudinal-mode PZT for CCFL applications

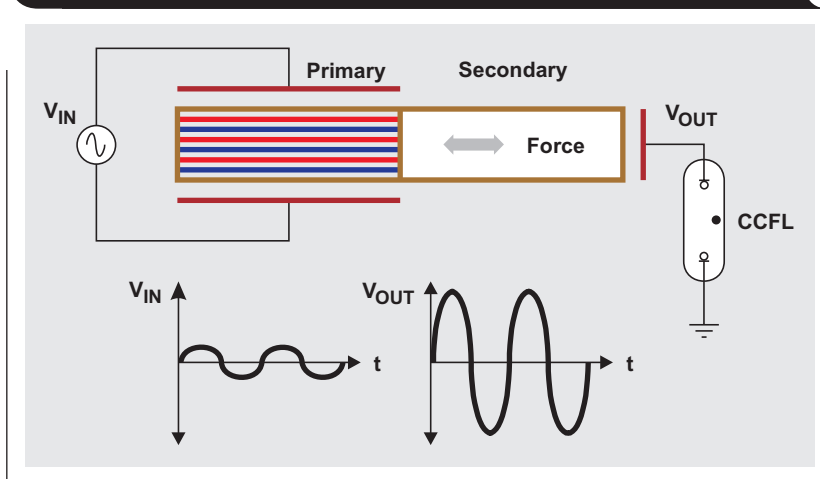


Figure 3 shows the typical construction for a Panasonic PZT (EFTU11R8Mx, EFTU14R0Mxx, and EFTI16R5Mxx series). Notice how the placement of the electrodes corresponds to that shown in Figure 2.

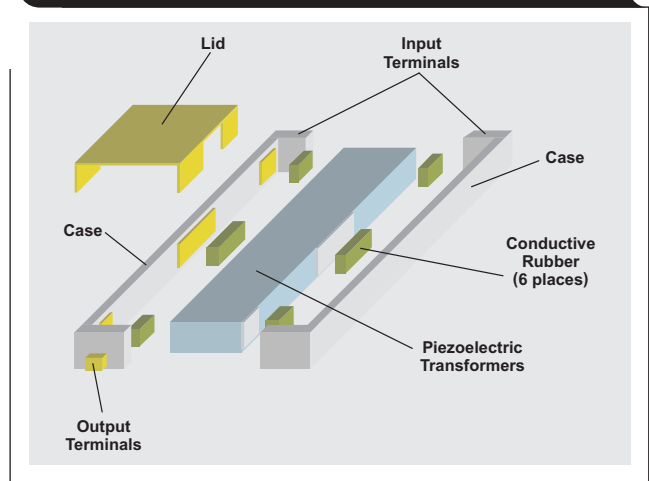
### PZT electrical model

To predict PZT performance in a system, it is useful to develop an electrical circuit model. The model shown in Figure 4 is often used to describe the behavior of a longitudinal-mode PZT near the fundamental resonant frequency. Many PZT manufacturers provide component values for the model based on measurements taken at various frequencies and output loads.

The component values depend on the PZT's construction and vary from one PZT part number to another. The input, or primary, capacitance ( $C_{INPUT}$ ) is formed as a result of the multilayer construction of the primary electrodes and material dielectric constant. This creates a relatively large input capacitance, much like a standard multilayer ceramic capacitor. The output capacitance,  $C_{OUT}$ , is much smaller due to the distance between the primary and secondary electrodes. As shown in the following equation, the PZT capacitance is a function of its geometry and material.

$$C_{INPUT} \approx \frac{\text{Length} \times \text{Width} \times \text{Layers} \times \epsilon}{2 \times \text{Thickness}}$$

**Figure 3. Typical construction of PZT (Panasonic's (EFTU11R8Mx, EFTU14R0Mxx, EFTI16R5Mxx series)**



The mechanical resonant frequency,  $\omega_0$ , of the PZT is also dependent upon geometry and material.

$$\omega_0 \propto \frac{1}{\text{Length}} \sqrt{\frac{Y}{\rho}}$$

where Y is the material elasticity and  $\rho$  is the material density.

The mechanical piezoelectric gain near a single resonant frequency is modeled by the series R, L, and C circuit as depicted in Figure 4.

$$\omega_0 = \frac{1}{\sqrt{L \times C}}$$

$$Q = \omega_0 \times \frac{L}{R}$$

Component values for a typical 1.8-W PZT (Panasonic part number EFTU11R8MX50) for Figure 4 are  $C_{INPUT} = 61.6 \text{ nF}$ ;  $C_{OUT} = 11.4 \text{ pF}$ ;  $n = 35$ ; and series RLC =  $0.66 \text{ } \Omega$ ,  $0.94 \text{ mH}$ , and  $2.79 \text{ nF}$ , respectively. The gain and the mechanical resonant frequency of the PZT change with load. These changes directly affect the electrical voltage gain. Figure 5 shows the graph of the electrical voltage gain versus frequency and load for the Panasonic PZT. It also shows that the PZT is capable of providing a large range of voltage gain. The PZT is operated near the 1-M $\Omega$  load line to provide the extremely high gain necessary to produce CCFL strike voltages. When loaded, it operates at a much lower gain to provide the lower operating voltages.

**Figure 4. Equivalent piezoelectric transformer circuit model**

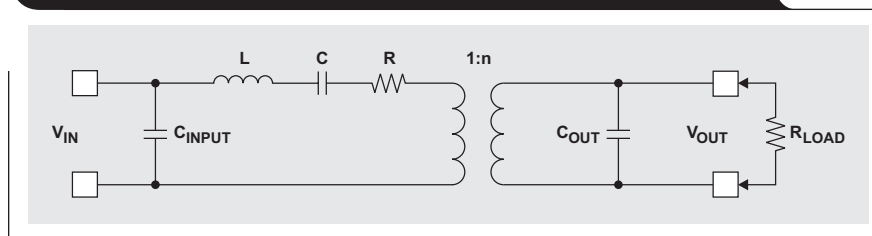
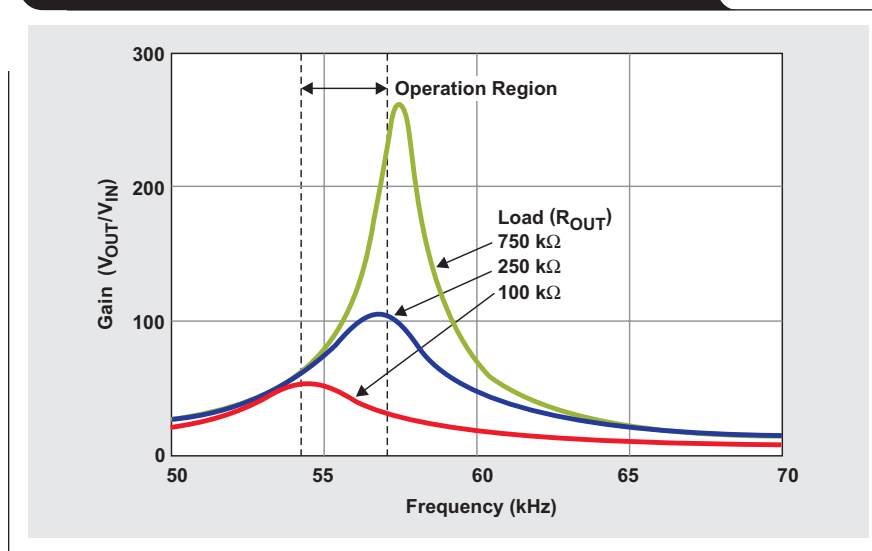


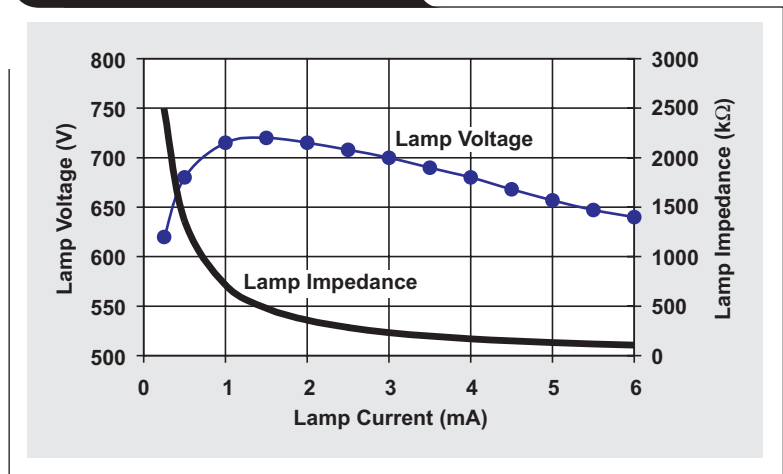
**Figure 5. Typical piezoelectric gain characteristics vs. frequency and load**



### CCFL lamp characteristics

Understanding the electrical operating characteristics of a CCFL is essential to understanding how to control its behavior. Before the lamp is ignited, it has an extremely high resistance and is modeled as an open circuit. The voltage required to ignite the lamp is called the strike voltage, which is dependent upon lamp length and diameter, is usually in the range of 500 to 2000 V. Strike voltage can be even higher at cold operating temperatures. When the lamp strikes, current begins to flow. The drop in operating voltage and the increase in current reduce the dynamic impedance of the CCFL. Figure 6 shows the nonlinear voltage and current characteristics of a typical CCFL. Although highly nonlinear, the lamp impedance can be modeled as a resistor at any one operating point. Lamp intensity is roughly proportional to lamp current.

Figure 6. CCFL characteristics

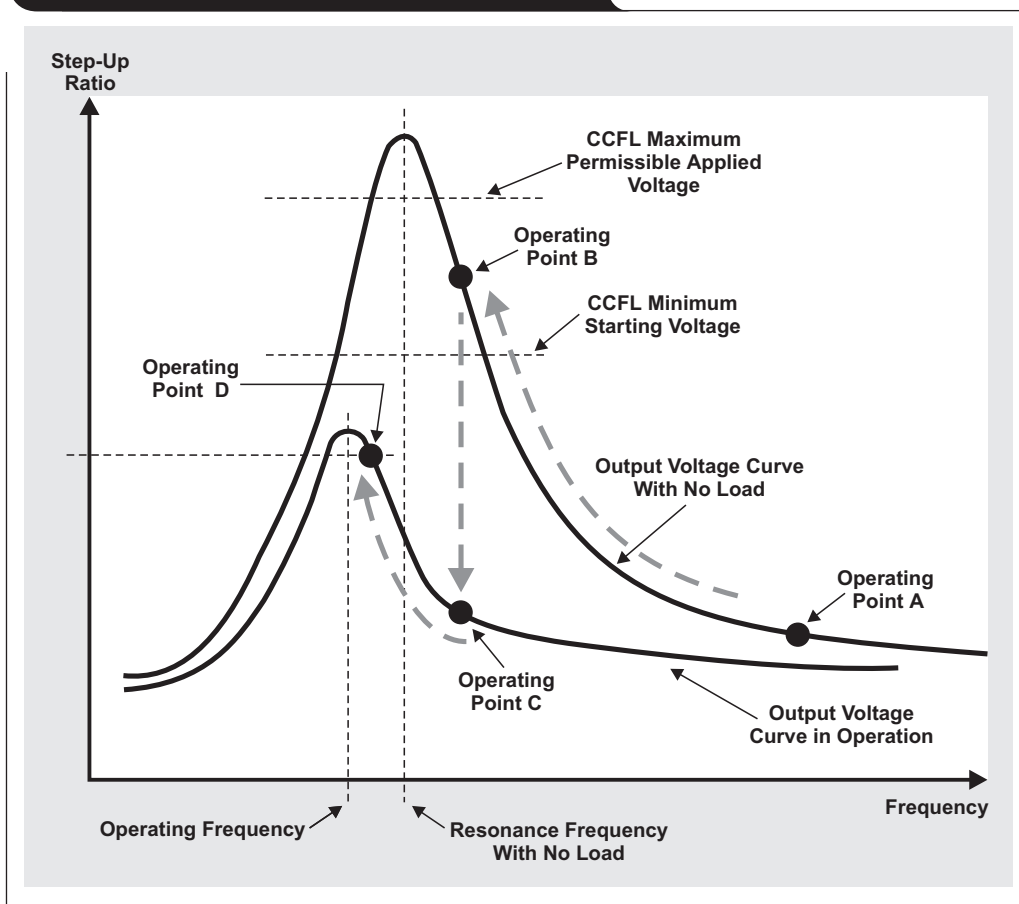


### CCFL/PZT interaction

Figure 7 shows the operational interaction between the CCFL and the PZT. Figure 7 is a combination of Figure 5 (PZT gain versus frequency and load) with Figure 6 (CCFL impedance versus current). Integrating Figures 5 and 6 and examining the result gives insight into the basic

operating principle of the CCFL backlight power-supply controller. At turn-on, the lamp is an open circuit, so the PZT operates on the high-gain, high-impedance load line shown in Figure 7. Since the exact strike voltage and operating frequency are not known, the controller applies

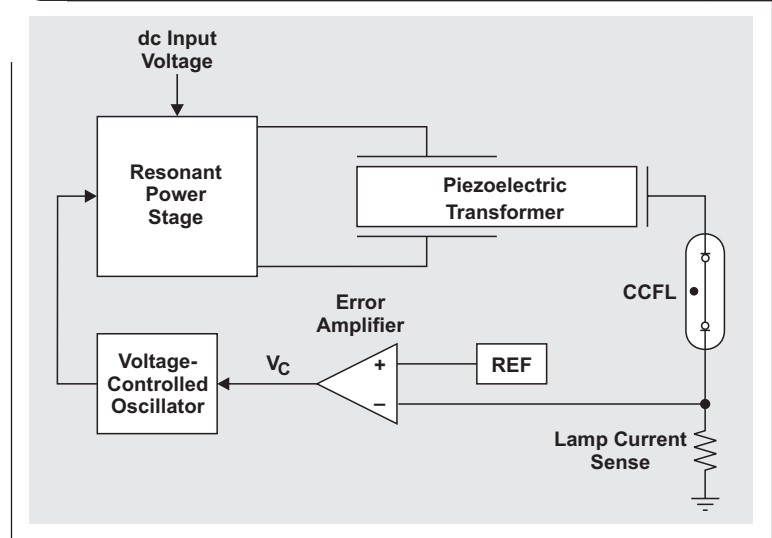
Figure 7. PZT with CCFL load operating points



a relatively low voltage to the lamp by operating at the maximum-programmed operational frequency. This is shown as Point A. As the operating frequency is decreased, the PZT gain moves up the no-load line until the CCFL strike voltage is reached. This is shown as operating Point B. At Point B, the CCFL strike voltage is reached and the lamp impedance begins to decrease. The operating frequency continues to decrease as the lamp impedance drops until the correct operating point is reached, somewhere between Points C and D. Varying the operating point between Points C and D controls the lamp intensity. This is accomplished by varying the operating frequency of the converter.

Figure 8 shows a simplified block diagram of a PZT-based backlight converter. The PZT is driven by a resonant power stage whose amplitude is proportional to input voltage. The PZT provides the voltage gain necessary to drive the lamp. A control loop is formed around the error amplifier that compares average lamp current to a reference signal, REF, allowing the intensity of the lamp to be regulated. The resulting control voltage,  $V_C$ , drives a voltage-controlled oscillator (VCO) that determines the operating frequency of the resonant power stage. The frequency range of the VCO must include the strike and operating frequencies of the PZT. For example, a frequency range of 51 to 71 kHz is required for proper operation of the lamp characteristics shown in Figure 5. The designer must guarantee that the PZT gain is sufficient to provide the required lamp voltage at minimum input voltage to keep the operating point on the right side of resonance. If the operating point crosses from the right side to the left side of resonance, the supply loses control of the lamp current and the lamp turns off.

**Figure 8. Control system for variable-frequency PZT backlight circuit**

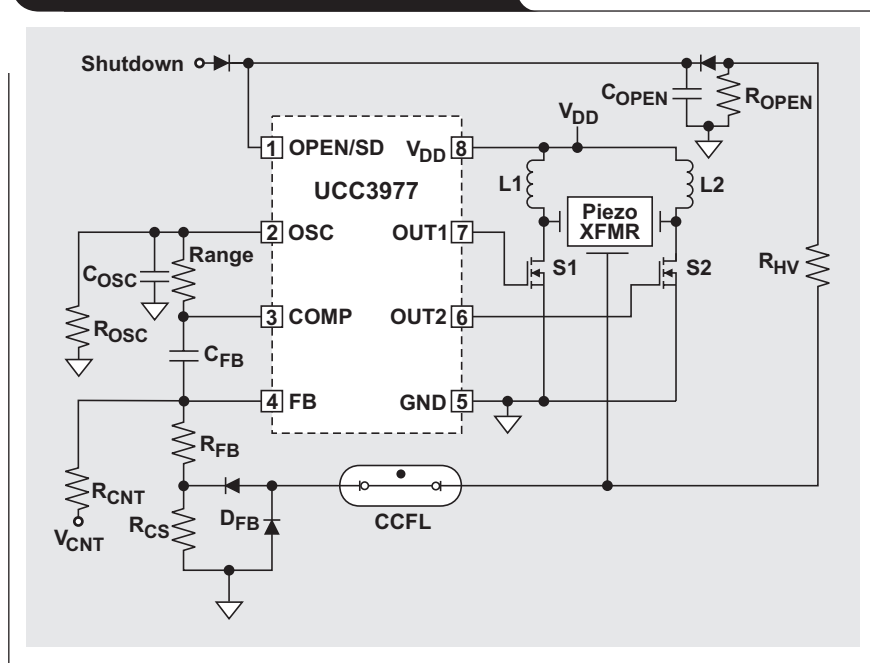


### Power topologies

Several topologies exist for the resonant power stage shown in Figure 8. Input voltage range, lamp characteristics, and PZT characteristics determine the correct resonant power stage topology. Some of the more popular choices are the push-pull, half bridge, and full bridge.

Figure 9 shows a basic resonant push-pull topology. The push-pull topology requires two external inductors but has the advantage of providing increased voltage across the PZT primary. This allows a lamp to be operated from a lower input voltage.

**Figure 9. Resonant push-pull topology**



The explanation of circuit operation is fairly simple. For the push-pull circuit, MOSFETs S1 and S2 are driven out of phase with 50% duty cycle at variable frequency (see Figure 10, trace 2). Inductors L1 and L2 resonate with the PZT primary capacitance, forming half sinusoids at the drain of S1 (trace 1) and S2 (trace 4). The resulting voltage across the PZT primary is a near sinusoid (trace M1). Due to the high Q of the ceramic transformer, the lamp voltage, which is approximately 600 V in this particular application, is sinusoidal (trace 3).

To achieve 0-V switching, each drain voltage must return to 0 V before the next switching cycle. This dictates that the LC resonant frequency be greater than the switching frequency. The maximum inductance to meet these conditions can be found from

$$L < \frac{1}{4\pi^2 f^2 C_{INPUT}}$$

where  $C_{INPUT}$  is the input capacitance of the transformer primary.

### PZT performance

High efficiency can be achieved by selecting the best power topology while matching the lamp, input voltage, and PZT characteristics. Figure 11 shows the performance of a 4-W-rated multilayer PZT operating a 600-V lamp with the push-pull topology at various input-voltage and lamp-current conditions. Electrical efficiency is greater than 85% at lower input voltages, decreasing at higher input voltages as the PZT gain is reduced. This circuit and lamp can operate from 2 Li-Ion cells (5 to 8.2 V). The same PZT and lamp would require 3 Li-Ion cells for a half-bridge topology but would yield similar efficiency.

Dimming by linearly reducing lamp current causes the efficiency to degrade, since the PZT is operated at less than optimal gain (see the 1.5-mA curve in Figure 11). Improved efficiency can be achieved by using burst-mode dimming. This dimming method involves running the lamp at full power but controlling average lamp current by modulating the on/off duty cycle at a frequency higher than the eye can detect (100 Hz, for example).

Figure 10. Push-pull waveforms

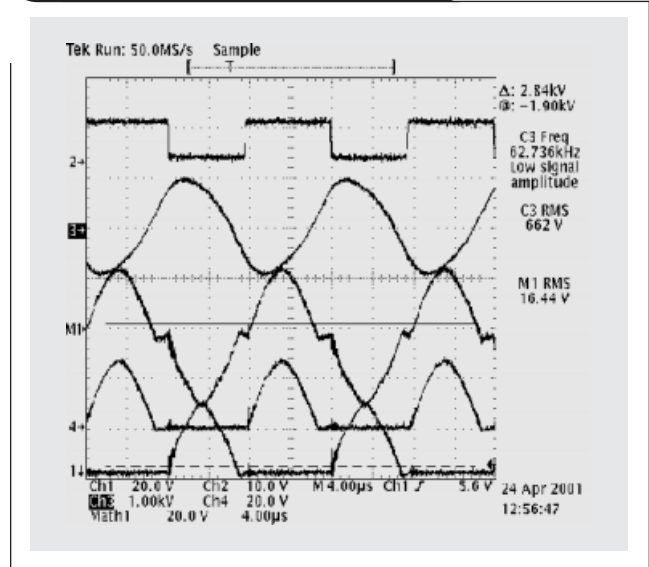


Figure 11. Typical PZT efficiency with input voltage and loading

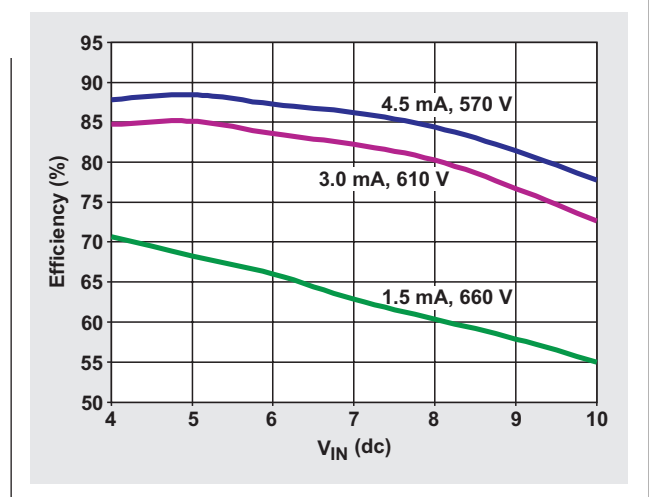


Figure 12 shows plots of PZT operating frequency over the same lamp conditions as Figure 11. As expected, frequency decreases at higher lamp currents as the PZT characteristics shift to a lower operating frequency when loaded (see Figure 5). Frequency increases linearly with input voltage, since the required  $V_{OUT}/V_{IN}$  gain to operate the lamp is decreased.

### Summary

Piezoelectric transformers offer several advantages for size-constrained, high-performance portable applications. Designing a backlight supply with PZT technology requires a basic understanding of PZT characteristics and performance. A push-pull power topology, along with its various merits for driving a PZT, has been presented. The operation

of longitudinal-mode PZTs in a variable-frequency control system has also been reviewed. A successful design will require matching the ceramic transformer to the application to attain high efficiency and stable performance. More information about the control ICs presented in this article can be obtained by contacting the author.

### Reference

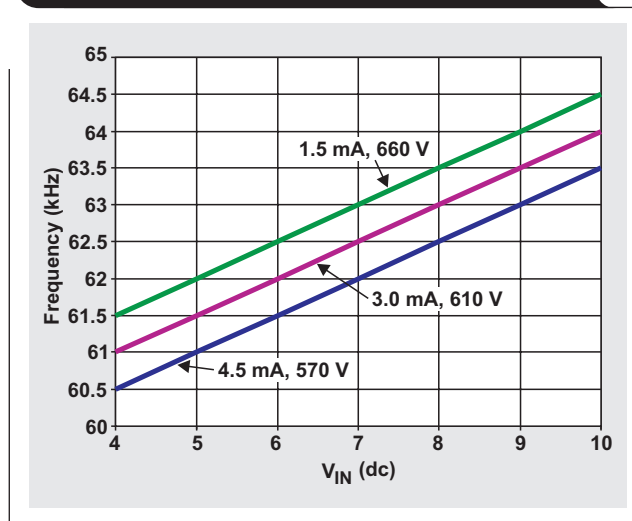
1. C.A. Rosen, "Ceramic Transformers and Filters," *Proceedings of the Electronic Components Symposium* (1956), p. 205.

### Related Web sites

[analog.ti.com](http://analog.ti.com)

[www.ti.com/sc/device/UCC3977](http://www.ti.com/sc/device/UCC3977)

**Figure 12. PZT operating frequency vs. input voltage and lamp load**



# Active output impedance for ADSL line drivers

By Randy Stephens (Email: r-stephens@ti.com)

Systems Specialist, Member Group Technical Staff

## Introduction

The exceptional bidirectional data transmission rates over traditional telephone lines are a major factor for the widespread industry growth of ADSL. The ability to transmit data at over 8 MBps over an existing infrastructure of copper telephone lines with limited costs is exciting. There are several key components within the ADSL system, but this article deals solely with the line driver amplifiers.

Because ADSL is considered to be a full-duplex system, able to transmit and receive at the same time, a receiver must be incorporated into the design. The most common way of accomplishing this is to use a hybrid network. The hybrid's function is to cancel out the transmit signal while still being capable of receiving the signals from the customer-premise equipment (CPE) end (also known as the remote-terminal [RT] end). To accomplish this task, series-matching resistors,  $R_S$ , are needed and should be equal to one-half the total reflected transmission line impedance to properly match the line impedances (see Figure 1).

$$R_S = \frac{R_{Line}}{2n^2}, \quad (1)$$

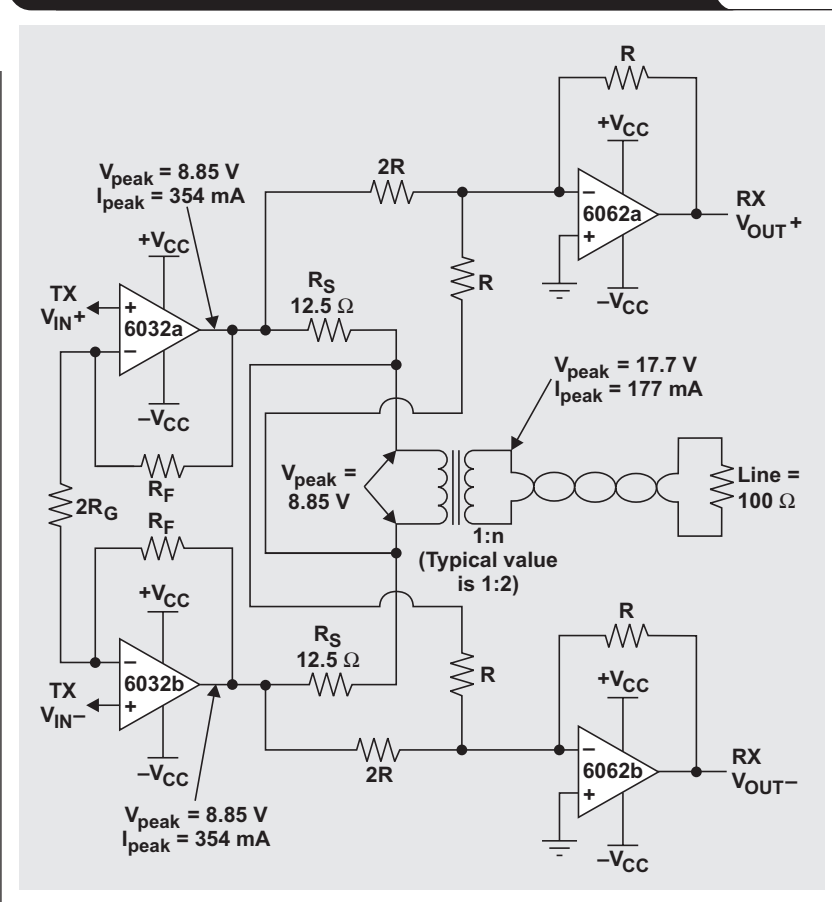
where  $n$  is the transformer ratio indicated as 1:n.

The problem with using the series-matching resistor is the associated voltage drop across this resistance. The voltage appearing at the transformer primary side is only one-half the voltage developed at the line driver amplifier output. This is one of the key issues when the power dissipation of an ADSL line driver is considered.

## Traditional line driver requirements

ANSI T1.413 specifies that the central office (CO) can nominally transmit at  $-40$  dBm/Hz on a  $100\text{-}\Omega$  telephone line from approximately 25 kHz to 1.104 MHz. This corresponds to roughly  $3.16 V_{RMS}$  (or  $+20$  dBm) being transmitted on the line. The problem is that ANSI T1.413 also dictates that there shall be a bit-error rate (BER) of  $1 \times 10^{-7}$ . In order to accomplish this feat the ADSL signal must have a peak-to-rms ratio, also known as crest factor (CF), of about 5.6 (15 dB). Taking the crest factor into account, the line voltage must now have a peak voltage of about  $17.7 V_{peak}$  ( $34.4 V_{pp}$ ). Note that the crest factor can vary

Figure 1. Line driver voltage and current levels to meet ANSI T1.413 requirements



from 5.3 to as high as 7, depending on the manufacturer and the system goals involved.

This large voltage requirement is a key reason for using a transformer and two amplifiers configured differentially to drive the line. Differential circuits have several advantages over single-ended configurations. This includes minimizing common-mode signals and interference, improving power-supply rejection, and the obvious advantage of doubling the voltage swing that appears at the transformer leads. Another advantage of the differential configuration is that even-order harmonics are reduced by as much as 10 to 20 dB, resulting in a very low distortion system.

Because  $R_S$  forces the amplifier to swing twice the transformer voltage requirement, the power supplies ( $\pm V_{CC}$ ) must be increased accordingly. This increase in power-supply voltage leads to the primary issue with ADSL line drivers—power dissipation.

## Line driver power dissipation

Power dissipation in the line driver amplifier is a dominant factor in CO applications. Let's take an approximation at the power dissipation levels required for the traditional line driver circuit. Let's assume that the amplifier requires at least 2 V of power-supply voltage headroom (i.e.,  $V_{OUT(max)} = V_{CC} - 2\text{ V}$ ) and there is about a 10% tolerance on the power supply. Since power dissipation of amplifiers is calculated based on the average current flowing into the amplifiers and the dc voltage, the following line driver amplifier power dissipation approximation can be made:

$$P_{Diss} = [2(V_{CC} - V_{OUT_{RMS}})(I_{OUT_{RMS}} \times 0.8^*)] + P_{Quiescent} \quad (2)$$

$$P_{Quiescent} \approx 4 \times V_{CC} \times I_{CC} \times 0.7 \quad ** \quad (3)$$

To solve for power dissipation, let

$$\begin{aligned} V_{CC(min)} &\approx V_{OUT(max)} + V_{Headroom} + V_{CC_{Tolerance}} \\ &= 8.85\text{ V} + 2\text{ V} + 1.1 = 11.94\text{ V} \\ &\quad (\text{choose standard voltage } 12\text{ V}_{DC}). \end{aligned}$$

$$V_{OUT_{RMS}} = 8.85\text{ V}_{peak} \div 5.6 = 1.58\text{ V}_{RMS}.$$

$$I_{OUT_{RMS}} = 354\text{ mA}_{peak} \div 5.6 = 63.2\text{ mA}_{RMS}.$$

$$\text{Let } I_{CC} = 12\text{ mA}_{DC}.$$

$$\therefore P_{Diss} \approx 1.05\text{ W} + 0.40\text{ W} \approx 1.45\text{ W}.$$

As you can see from the calculation, 1.45 W is a lot of power for a single device to dissipate. To compound the problem, there are as many as 72 ADSL lines on a single PCB. This is an enormous amount of heat to try to dissipate while trying to maintain proper silicon die temperatures.

## Minimizing power dissipation

Power reduction is easily accomplished by reducing the series-matching resistors ( $R_S$ ) to a much smaller value. The voltage drop across these resistors is then minimized. The amplifier output voltage is reduced by the same amount that allows the power-supply voltages to be reduced. Because the voltage difference between the power-supply voltage and the rms output voltage is reduced, power dissipation is also reduced. The quiescent power is reduced as well, due to the dropping power-supply voltages. Using the previous example, we can see the amount of power that will be saved by simply utilizing a smaller resistor. Let new  $R_S$  equal 13% of the original  $R_S$  value.

$$\text{New } V_{OUT(max)} = 1.13 \times \text{old } V_{OUT(max)} \div 2 = 5\text{ V}.$$

$$\begin{aligned} \text{New } V_{CC} &= (5\text{ V} + 2\text{ V}) \times 1.1 = 7.7\text{ V} \\ &\quad (\text{choose standard voltage } 8\text{ V}_{DC}). \end{aligned}$$

\* The ADSL signal is considered to have a Gaussian distribution in the time domain. Because of this, multiplying the amplifier's rms output current by approximately 0.8 yields the average current drawn from the power supply due to the output signal current.

\*\* This multiplication factor accounts for the fact that part of the quiescent current in a Class-AB amplifier gets diverted to the load when there is a signal appearing at the output of the amplifier driving a load. The number chosen is only an approximation and is shown only as a reference. Typical numbers range from 0.4 to 0.9 and are based on numerous circuit parameters internal to the amplifier.

$$\text{New } V_{OUT_{RMS}} = 5\text{ V} \div 5.6 = 0.893\text{ V}.$$

$$\text{New } I_{OUT_{RMS}} = \text{old } I_{OUT_{RMS}} = 63.2\text{ mA}.$$

$$\therefore \text{New } P_{Diss} \approx 0.72\text{ W} + 0.22\text{ W} \approx 0.94\text{ W}.$$

This is a savings of 0.51 W, or 35%, per ADSL channel. When there are several channels on a single PCB, this can add up to substantial heat savings. The die temperature is also reduced, allowing for better performance and longer life of the amplifier.

However, this configuration fails to allow for proper line impedance matching. To get the best of both worlds, utilizing small series resistors and matching the line impedance, we need to use an "old" circuit configuration—the active termination circuit (also known as synthesized impedance).

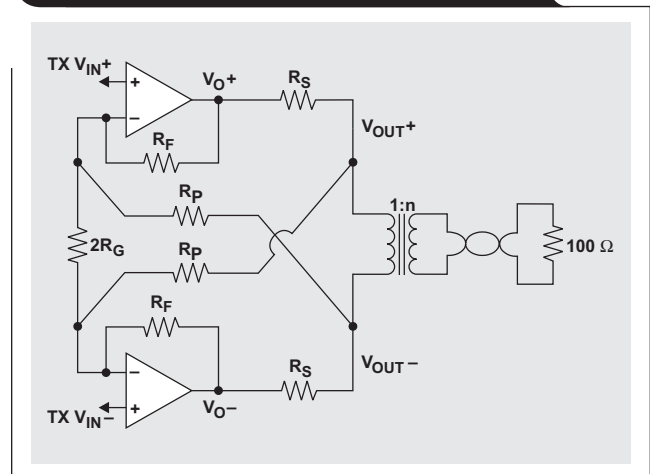
## Active termination

Active termination has been around for several years.<sup>1,2</sup> The idea is to use a small ohmic value resistor for  $R_S$ . The circuit then utilizes positive feedback to make the impedance of this resistor appear much larger from the line side.

This accomplishes two things: (1) a very small resistance when the line driver amplifier transmits signals to the line, and (2) proper matching impedance between the line and the amplifier. Most of the original designs, however, were single-ended applications instead of the differential configuration used in ADSL systems.

Taking the general idea a step further, we can utilize the fact that the signals from each amplifier are 180° out of phase from each other in the differential system. We use these signals and connect them into the traditional inverting node on the amplifier (minus input) instead of the non-inverting node (plus input) used in the single-ended application. The advantages of this are: (1) The effective impedance of the noninverting inputs is not dictated by the positive feedback resistance and voltage gain; and (2) the active impedance achieves cross-coupling of the signals. Cross-coupling helps minimize differences between the two amplifier output signals, helping to keep the signals fully differential. Figure 2 shows the basic circuit for differential positive feedback.

Figure 2. Basic active impedance circuit



The first question to answer is: How does this circuit configuration increase the effective resistance of  $R_S$  when looking from the line? If we assume that the TX inputs are grounded and apply a voltage at  $V_{OUT-}$ , this creates a voltage at  $V_{O+}$  equal to  $V_{OUT-} \times -R_F/R_P$ . If we also realize that the voltage at  $V_{OUT+}$  is equal to  $-V_{OUT-}$ , then  $V_{O+} = V_{OUT+} \times R_F/R_P$ . This makes  $R_S$  appear to be a larger impedance,  $Z$ , by the following formula:

$$Z(\Omega) = \frac{R_S}{1 - \frac{R_F}{R_P}} \quad (4)$$

The important thing to consider is that regardless of the forward gain from  $V_{IN}$  to  $V_O$ , the active impedance value remains constant. The drawback to this arrangement is that the impedance will change at frequencies near the amplifier's bandwidth limit. We must ensure that the amplifier used has a bandwidth high enough not to alter the impedance at the ADSL frequencies from 25 kHz to 1.1 MHz. As a general rule of thumb, the amplifier must have a minimum bandwidth of 10 times the maximum operating frequency, or at least 11 MHz with the amplifier's intended gain.

### Active impedance forward gain

Once the return impedance is corrected, we need to turn our attention to the rest of the design parameters. The most fundamental is the forward voltage gain from input to output. For simplicity, we will assume that the amplifier is well within its linear range and ignore bandwidth effects. Equation 5 shows the simplified forward gain from  $V_{IN}$  to  $V_O$ .

$$A_V = \frac{V_{O\pm}}{V_{IN\pm}} = \frac{1 + \left( \frac{R_F}{R_G \parallel R_P} \right)}{1 - \left( \frac{R_F}{R_P} \right) \left( \frac{R_L}{R_L + R_S} \right)} \quad \text{if } R_L \ll R_P, \quad (5)$$

$$\text{where } R_L = \frac{R_{Line}}{2n^2}. \quad (6)$$

In the original circuit (the classic design shown in Figure 1),  $R_S$  equaled one-half the total reflected line impedance, which also equaled  $R_L$ . We must now choose  $R_S$  as a percentage of  $R_L$  in the active termination circuit. If we define the variable  $X$  as this percentage, where  $0 < X \leq 1$ , then we can start simplifying the preceding equations. Some references use the term "synthesis factor" (SF) to describe the percentage. Synthesis factor is simply  $1/X$ , but the remainder of this article uses the variable  $X$ . If we realize that the term

$$\frac{R_L}{R_L + R_S}$$

is held constant, we can make several simplifications. The first sets of assumptions are

$$R_S = R_L X \quad \text{and} \quad (7)$$

$$\frac{R_L}{R_L + R_S} = \frac{1}{1 + X}. \quad (8)$$

We will also assume that we want the active impedance,  $Z$ , equal to the terminating resistance,  $R_L$ . Equation 4 is manipulated to achieve

$$R_P = R_F \left( \frac{1}{1 - X} \right) = \frac{R_F}{1 - X}. \quad (9)$$

Equation 9 shows that to properly match the active termination impedance, we need only select an arbitrary value of  $R_F$ . Substituting Equations 7 through 9 in Equation 5 leads us to the simplified forward voltage gain of

$$A_V = \frac{R_G[(1 + X)(2 - X)] + R_F(1 + X)}{2R_G X}. \quad (10)$$

If we know the forward gain we want in the system, we can rearrange Equation 10 to solve for the gain resistance,  $R_G$ :

$$R_G = \frac{R_F(1 + X)}{2A_V X - [(1 + X)(2 - X)]}. \quad (11)$$

### Minimum active impedance forward gain design constraint

Because active impedance utilizes positive feedback, it is possible to create negative impedance instead of positive impedance. Negative impedance makes the series resistance appear to decrease rather than to increase as desired; so we must ensure that there is always positive impedance. We come to our first design constraint of the active termination circuit: There must be a minimum forward gain for the system to work properly.

Because we want to match the line properly, we must first arbitrarily choose  $R_F$ . Using Equation 9 dictates a specific fixed value for  $R_P$ . This leads to  $R_G$  solely dictating the forward voltage gain for any given value of  $X$ . The minimum forward voltage gain allowed is when  $R_G$  is not even in the system, resulting in

$$A_{V(\min)} = \frac{2 + X - X^2}{2X} = \frac{(1 + X)(2 - X)}{2X}. \quad (12)$$

Luckily, for most ADSL systems, the gain of the amplifiers is typically greater than 10 V/V. Meeting the minimum gain requirement is usually not an obstacle as long as the value of  $X$  is greater than about 10%. As long as the minimum forward gain is met, the low-power active termination system will work properly.

### Line impedance changes

Up until now, we have assumed that the line was a fixed value (usually 100  $\Omega$ ). But in reality, we know that the line impedance is highly complex. Typically the line impedance can range from as low as 50  $\Omega$  up to as high as 300  $\Omega$  over the ADSL frequency spectrum. Since the positive feedback

is obtained between  $R_S$  and the reflected line impedance ( $R_L$ ), it stands to reason that the forward voltage gain will be affected.

To quantify the exact change in forward voltage gain, the variable  $Y$  is introduced. Let the variable  $Y$  equal the percentage change in the reflected line impedance ( $R_L$ ). This leads to the new forward voltage gain:

$$A_V = \frac{R_G[(2-X)(1+X+Y)] + R_F(1+X+Y)}{R_G X(2+Y)} \quad (13)$$

Figure 3 illustrates the percentage change in forward gain with varying values of  $X$ . The forward gain with a 100- $\Omega$  line impedance will be used as the base line for comparison.

It is interesting to note that the change in percentage gain is independent of the transformer ratio,  $n$ ; feedback resistance,  $R_F$ ; gain resistance,  $R_G$ ; and initial amplifier gain,  $A_V$ .

The minimum forward gain will also vary with the line impedance. The minimum forward gain becomes

$$A_{V(\min)} = \frac{(2-X)(1+X+Y)}{X(2+Y)} \quad (14)$$

Figure 4 illustrates the minimum forward gain with varying line impedance.

When an active termination system is designed, it does not matter what initial design line impedance is used. As

long as the minimum gain criterion is met, the system should not create negative impedances.

### Line impedance changes and the amplifier output voltage

In a real system it is quite common for forward voltage gain to change  $\pm 20\%$ , which must be accounted for. If not, the input signal can be amplified too high and clipping could easily occur. Excess distortion, data transfer rate, line reach, and even power dissipation could become worse if the line impedance is not handled properly within the active impedance circuit design.

Examining the circuit of Figure 2 and using Equation 7 will help us calculate how the line impedance changes the amplifier's output voltage. We will assume that  $R_S$  is designed for a 100- $\Omega$  system and is held constant. We will also assume that the power on the line was done with a 100- $\Omega$  line impedance and is +20 dBm. This corresponds to a line voltage of 3.162  $V_{RMS}$ . The formula used to find the corresponding amplifier voltages is

$$V_{O_{RMS}} = \frac{V_{Line_{RMS}}(R_{Line} + 2n^2R_S)}{2nR_{Line}} \quad (15)$$

The important number is the peak output voltage of the amplifier ( $V_{peak} = V_{RMS} \times CF$ ) because a given supply voltage determines how much voltage swing can occur. Failure to plan for varying line impedances can cause

**Figure 3. Forward gain change with varying line impedance**

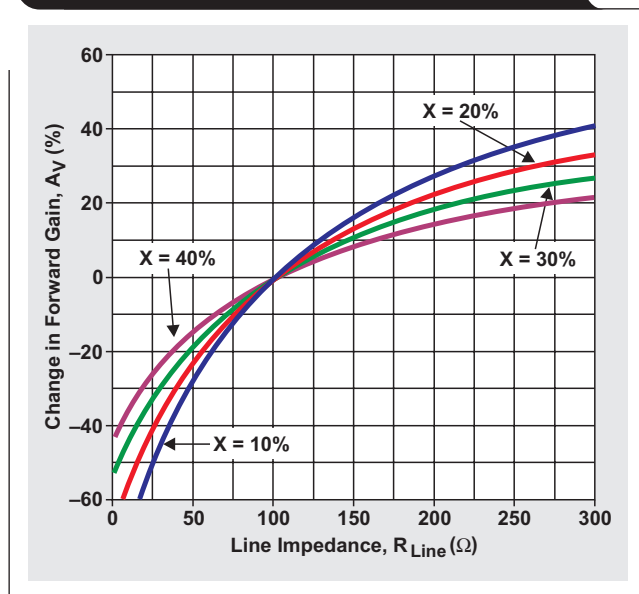
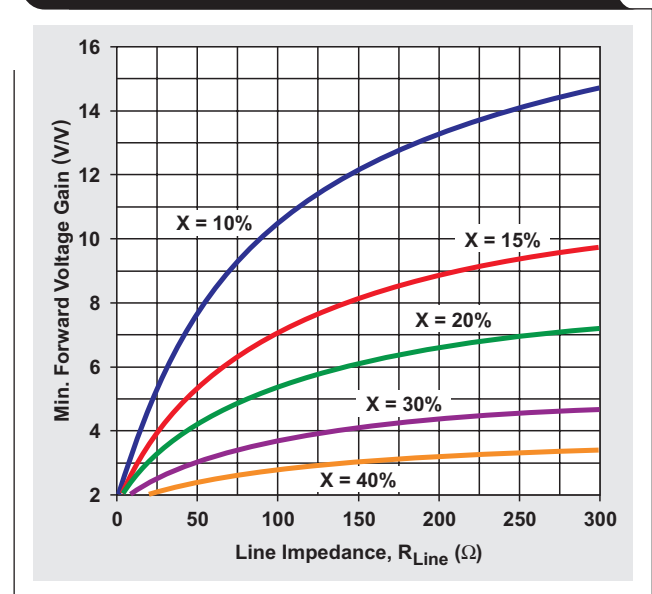


**Figure 4. Minimum forward gain change with varying line impedance**



some serious problems. Figure 5 illustrates this issue with  $X = 20\%$  ( $SF = 5$ ) and a crest factor of 5.3.

Obviously, as the crest factor increases, the peak output voltage will also increase. Additionally, when  $R_S$  increases, the amplifier output voltage will also increase. The obvious question is: Why not use the smallest resistance possible? There are several reasons for this that the remainder of this article explains in detail.

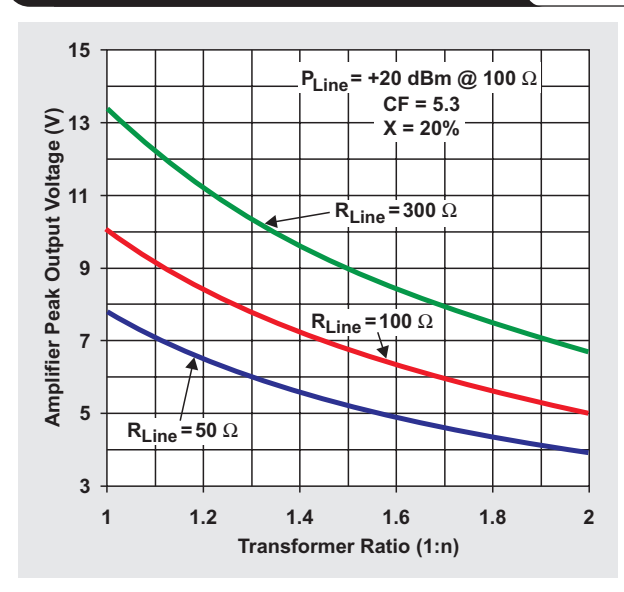
### Lab tests

#### Setup

The first test examined how the resistor values affect the system. Because the THS6032, like most ADSL line drivers, is a current feedback (CFB) amplifier, the feedback resistance ( $R_F$ ) dictates the bandwidth and the stability of the amplifier. Keeping a high bandwidth increases the amplifier's excess open-loop gain in the ADSL frequency band and reduces distortion. At the same time, however, the amplifier bandwidth may be high enough to interact with the transformer's resonance frequency, which can cause possible instabilities in the overall system. This is especially true when active impedance circuits are used, as  $R_S$  can become very small, resulting in very little isolation between the amplifier and the transformer. When you consider Equations 13 to 15 along with the transformer's impedance at resonance, it is apparent that the system can potentially become unstable. Using a simple RC snubber across the transformer can be a simple solution for instability concerns.

To circumvent this potential issue, two new amplifiers from Texas Instruments, the THS6132 and the THS6182, incorporate special internal circuitry. These new amplifiers yield extremely low distortion at the ADSL frequencies yet have a bandwidth of only 10 to 20 MHz—depending on the system design. For all other line drivers, the trade-off of bandwidth and stability needs to be managed. As a side benefit of reducing the feedback resistor, the overall output noise of the line driver system can be significantly reduced.

**Figure 5. Amplifier peak output voltage with  $X = 20\%$**



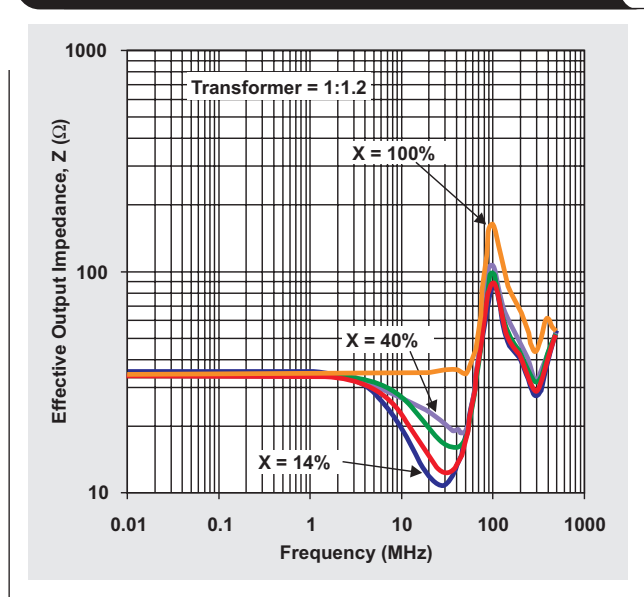
For the THS6032 testing, a feedback resistor value of  $1150 \Omega$  was chosen. The rest of the system component values were then easily calculated with the previous equations. The only other variable was that the gain of each amplifier was set to approximately  $+12 \text{ V/V}$ . This allowed testing of the  $X = 10\%$  system where the appropriate minimum gain requirement was about 10.5. As  $R_S$  was increased, the gain also had to be increased to account for the additional voltage drop from the added series resistance.

#### The active impedance test

Figure 6 shows the impedance looking back into  $R_S$  from the transformer primary. It clearly shows the amplifier's closed-loop bandwidth effects. Eventually the amplifier's own output impedance takes over regardless of the termination system used. At this point the impedance is out of the designer's control. Since the ADSL spectrum is well controlled, the system will meet its designated functionality as a low-power line driver.

One area of concern with using active impedance is that lightning surge tests could overwhelm the amplifiers' internal circuitry and cause failures due to a decreased real resistance between the amplifier and the transformer. The larger the resistance, the better the chance that no damage will occur within the amplifier. If the active impedance configuration is utilized, then  $R_S$  should be a "respectable" value and not something trivial (for example,  $1 \Omega$ ). Most systems should strive for a value of 20 to 30% of  $R_L$  ( $SF = 3$  to  $5$ ). This allows for respectable power savings and reasonable isolation from surges on the line.

**Figure 6. Amplifier effective output impedance viewed from transformer primary winding**



### Power dissipation and distortion

The line impedance used in the testing was a 100- $\Omega$  resistor. Variable line impedance issues are not of concern but should constrain the final system design. As a result, the power dissipation numbers shown should be considered optimal for a particular test setup. When a varying line impedance is thrown into the mix, the power-supply voltages will need to be adjusted accordingly and the power dissipation will increase.

The other factor hampering the power dissipation is that the THS6032 requires 4-V headroom from the power supplies. This is due to the Class-G architecture requiring multiple series transistors in the output stage. If a very low headroom amplifier were used (such as the THS6132 or THS6182), the power-supply voltage could be reduced by at least  $\pm 2$  V, decreasing power even more. As we are concerned with power savings in general, these results can be used to draw some general conclusions about the use of active termination in an ADSL application.

Keep in mind that when you compare power numbers from amplifier to amplifier, the entire system configuration needs to be divulged. This includes things such as crest factor; accounting for varying line impedances; accounting for power-supply tolerances; and, of course, the synthesis factor. Because of the numerous options available, doing a true apples-to-apples comparison is often very difficult when you just look at manufacturers' data sheets.

As a reference for the active termination testing, a THS6032 was tested with the traditional configuration

shown in Figure 1. To really see the effects of the Class-G circuitry in action, refer to Figure 7, which shows how changing the  $V_{CC-L}$  supply voltages alters the power dissipation. For reference, it also shows the power consumed in each set of supplies. In Class-AB mode, power dissipation is about 1.8 W; but in Class-G mode, the best power achieved is approximately 1.35 W with  $V_{CC-L}$  at  $\pm 6$  V. The multitone power ratios (MTPRs) were  $-70$  dBc for Class-AB operation and  $-68$  dBc for Class-G operation.

Figure 8 shows how the crest factor affects power dissipation with a 1:1.2 transformer and  $X = 20\%$  ( $R_S = 6.94 \Omega$ ). The power-supply voltage was chosen to give an additional  $\pm 0.5$ -V headroom for a design margin. In the lab, we could set the supplies  $\pm 1$  V lower before clipping started to occur; but this is not considered good practice, as power-supply tolerances and component tolerances could come into play. The power dissipation numbers shown are thus considered to be realistic and within the safe operating area of the system.

When compared to the traditional circuit design, the active termination circuit saved a huge 47% in power dissipation. This was true for both Class-AB operation and Class-G operation. For the active termination data, the use of Class-G operation saved an additional 20 to 25% power dissipation compared to the Class-AB operation. As expected, when the crest factor increased, the power dissipation also increased by as much as 25%. This was mainly due to the increase in power-supply voltage required to handle the larger peak voltages.

Figure 7. Traditional circuit design power dissipation results

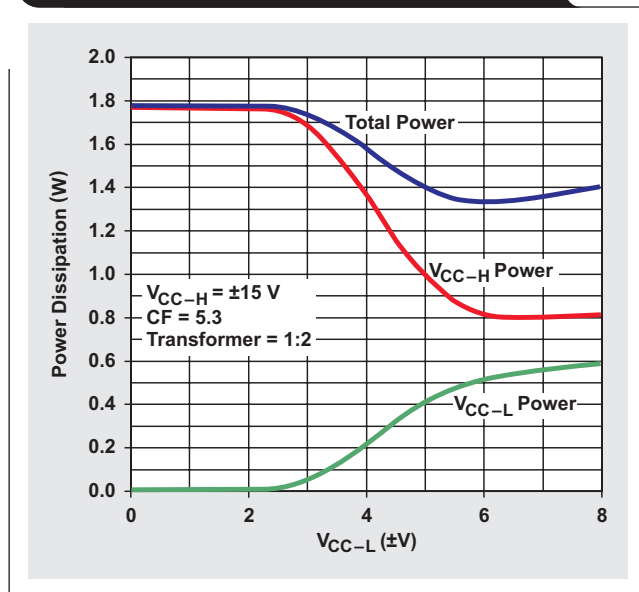


Figure 8. Power dissipation with 1:1.2 transformer and different crest factors

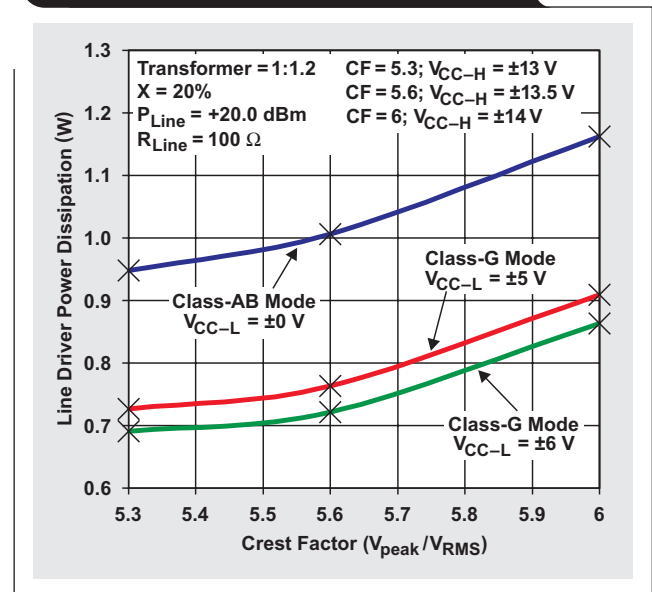


Figure 9 shows how changing  $R_S$  affects the power dissipation. A common crest factor of 5.3 was used to illustrate the change in the system.

If the power-supply voltages had been held constant and no clipping had occurred, the power dissipation would have decreased with an increase in  $R_S$ ; but the testing was done to show the best possible performance with a given set of constraints. The power-supply voltages thus were increased as  $R_S$  was increased to compensate for the increase in output voltage required from the amplifier. The power-supply voltages ranged from  $\pm 12.5$  V ( $X = 14\%$ ) to  $\pm 14$  V ( $X = 40\%$ ).

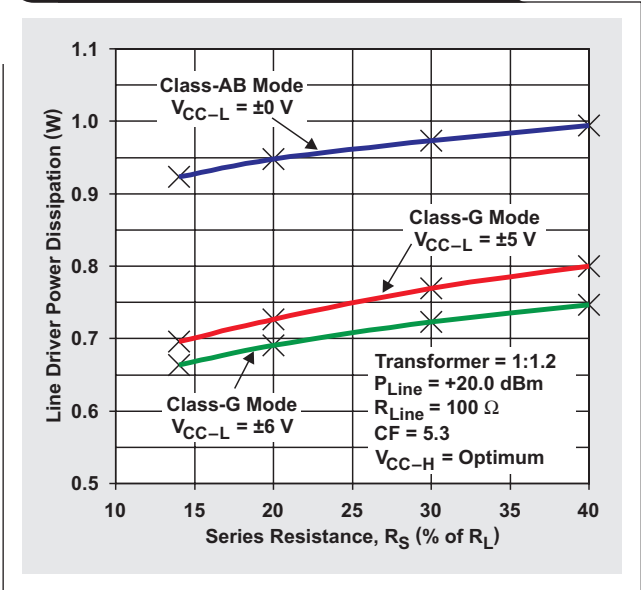
The last thing to check was the effect of MTPR distortion on the system.

Figure 10 shows us that as  $R_S$  increases, the MTPR distortion decreases. The designer has to choose between lower distortion and lower power dissipation. As stated earlier, a series resistance of 20 to 30% of  $R_L$  should give good results for both requirements.

**Power dissipation and MTPR with multiple transformer ratios**

The purpose of the next series of tests was to find out if there is a general relationship between the transformer ratio and the power dissipation. For each transformer ratio tested, the corresponding resistor values and power-supply voltages were accordingly changed. Figure 11 shows how changing  $R_S$  affects power dissipation with varying transformer ratios.

**Figure 9. Power dissipation with 1:1.2 transformer and varying  $R_S$**



Regardless of the power-supply voltages and the mode of operation, as  $R_S$  increases, the power dissipation increases. This is generally dominated by the amplifier's overhead

**Figure 10. MTPR with 1:1.2 transformer and varying  $R_S$**

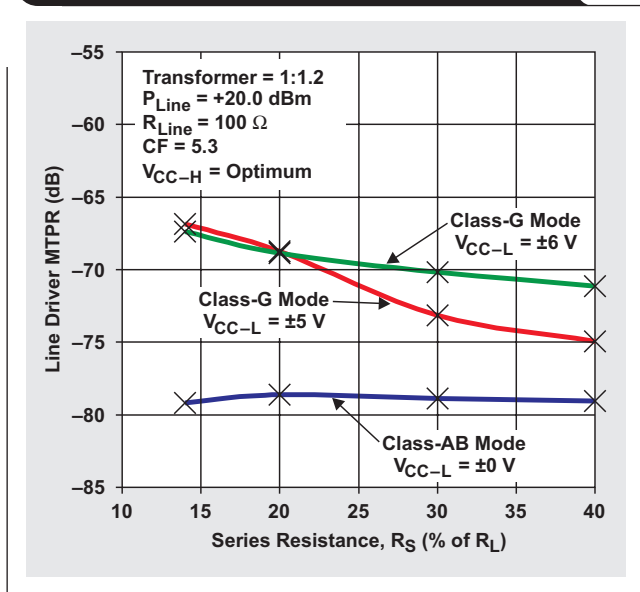
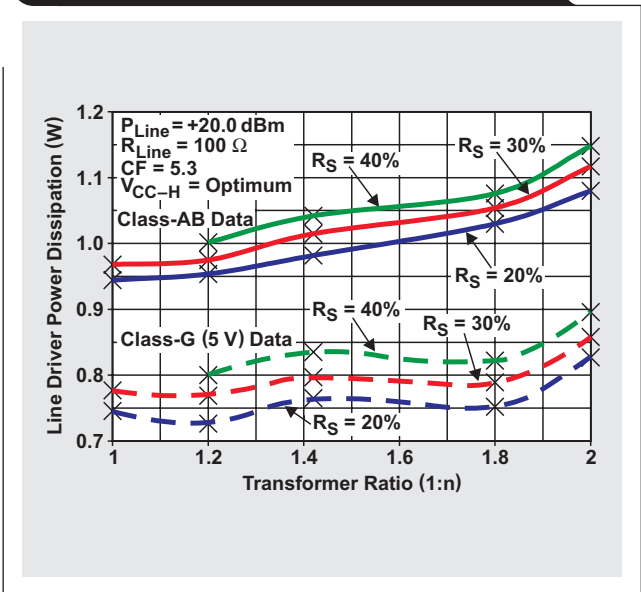


**Figure 11. Power dissipation with varying transformer ratios**



voltage requirements and quiescent current. We now come to the final test—determining the effects of varying transformer ratios on MTPR distortion. Figure 12 shows the effects of  $R_S$  on MTPR distortion with a changing transformer ratio and the same setup that was used before.

The data tells us that increasing the physical value of  $R_S$  lowers MTPR distortion. This is because distortion in operational amplifiers generally gets better with an increase in load resistance. In the case of the ADSL configuration, increasing  $R_S$  also helps isolate the complex loading that the transformer places on the amplifier. Comparing the 1:2 transformer data with the traditional circuit design shows that MTPR performance degrades by 4 to 5 dB as the transformer ratio increases.

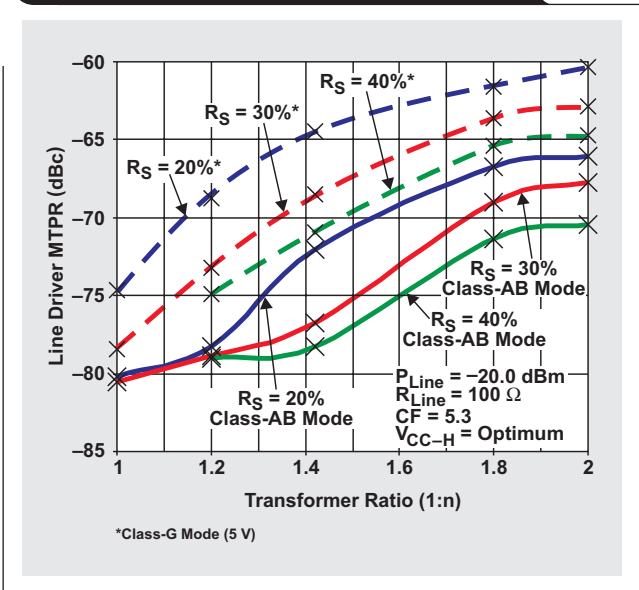
## Conclusion

Reduced power dissipation is the main goal for using active termination in ADSL systems. Using a 1:1.2 transformer saved 47% of power regardless of the mode in which the THS6032 was used. This translates to a savings of up to 0.85 W with Class-AB operation and 0.63 W with optimal Class-G operation. In light of the distortion and power savings, choosing a value for X of 0.2 to 0.3 (SF = 3 to 5) shows about the best overall performance.

Using TI's newest amplifiers, THS6132 (Class-G) or THS6182 (Class-AB), can save substantially even more power. Initial testing with the THS6132 in Class-G operation shows a total power consumption of as low as 0.53 W, which is a power dissipation of roughly 0.43 W over the THS6032. However, keep in mind the design constraints of the active termination system. The line impedance variations, the minimum power-supply voltages, and the system crest factor all contribute to the power consumption of the line driver.

With any electrical circuit, there are trade-offs to using one configuration over another. The active impedance circuit is no exception. The trade-off to achieving lower line driver power dissipation is that the receiver circuitry will require more voltage gain to overcome the voltage reduction appearing across  $R_S$ . This can play a significant role in the noise performance of the system. One way to help alleviate this problem is to use a smaller transformer ratio; but the power-supply voltages will have to be increased, which can increase power dissipation. The added benefits of an increased series resistance can help in many other areas of the system, including distortion and

Figure 12. MTPR distortion with varying transformer ratios



surge isolation. Ultimately, the goal of saving power can still be met while satisfying all requirements of the ADSL line driver system.

Additional information will be available in an application note to be released by January 2003, at [www-s.ti.com/sc/techlit/sloa100](http://www-s.ti.com/sc/techlit/sloa100)

## References

1. Jerry Steele, "Ideas For Design - Positive Feedback Terminates Cables," *Electronic Design* (March 6, 1995), pp. 91-92.
2. Donald Whitney Jr., "Design Ideas - Circuit Adapts Differential Input to Drive Coax," *Electronic Design News* (May 8, 1997), pp. 132-34.

## Related Web sites

[analog.ti.com](http://analog.ti.com)

[www-s.ti.com/sc/techlit/sloa100](http://www-s.ti.com/sc/techlit/sloa100) (available January 2003)

[www.ti.com/sc/device/partnumber](http://www.ti.com/sc/device/partnumber)

Replace *partnumber* with THS6032, THS6132 or THS6182

# Index of Articles

Title	Issue	Page
<b>Data Acquisition</b>		
Aspects of data acquisition system design	August 1999	1
Low-power data acquisition sub-system using the TI TLV1572	August 1999	4
Evaluating operational amplifiers as input amplifiers for A-to-D converters	August 1999	7
Precision voltage references	November 1999	1
Techniques for sampling high-speed graphics with lower-speed A/D converters	November 1999	5
A methodology of interfacing serial A-to-D converters to DSPs	February 2000	1
The operation of the SAR-ADC based on charge redistribution	February 2000	10
The design and performance of a precision voltage reference circuit for 14-bit and 16-bit A-to-D and D-to-A converters	May 2000	1
Introduction to phase-locked loop system modeling	May 2000	5
New DSP development environment includes data converter plug-ins (PDF - 86 Kb)	August 2000	1
Higher data throughput for DSP analog-to-digital converters (PDF - 94 Kb)	August 2000	5
Efficiently interfacing serial data converters to high-speed DSPs (PDF - 80 Kb)	August 2000	10
Smallest DSP-compatible ADC provides simplest DSP interface (PDF - 120 Kb)	November 2000	1
Hardware auto-identification and software auto-configuration for the TLV320AIC10 DSP Codec — a “plug-and-play” algorithm (PDF - 105 Kb)	November 2000	8
Using quad and octal ADCs in SPI mode (PDF - 94 Kb)	November 2000	15
Building a simple data acquisition system using the TMS320C31 DSP (PDF - 235 Kb)	February 2001	1
Using SPI synchronous communication with data converters — interfacing the MSP430F149 and TLV5616 (PDF - 182 Kb)	February 2001	7
A/D and D/A conversion of PC graphics and component video signals, Part 1: Hardware (PDF - 191 Kb)	February 2001	11
A/D and D/A conversion of PC graphics and component video signals, Part 2: Software and control	July 2001	5
Intelligent sensor system maximizes battery life: Interfacing the MSP430F123 Flash MCU, ADS7822, and TPS60311	First Quarter, 2002	5
SHDSL AFE1230 application	Second Quarter, 2002	5
Synchronizing non-FIFO variations of the THS1206	Second Quarter, 2002	12
Adjusting the A/D voltage reference to provide gain	Third Quarter, 2002	5
MSC1210 debugging strategies for high-precision smart sensors	Third Quarter, 2002	7
Using direct data transfer to maximize data acquisition throughput	Third Quarter, 2002	14
Interfacing op amps and analog-to-digital converters	Fourth Quarter, 2002	5
<b>Power Management</b>		
Stability analysis of low-dropout linear regulators with a PMOS pass element	August 1999	10
Extended output voltage adjustment (0 V to 3.5 V) using the TI TPS5210	August 1999	13
Migrating from the TI TL770x to the TI TLC770x	August 1999	14
TI TPS5602 for powering TI's DSP	November 1999	8
Synchronous buck regulator design using the TI TPS5211 high-frequency hysteretic controller	November 1999	10
Understanding the stable range of equivalent series resistance of an LDO regulator	November 1999	14
Power supply solutions for TI DSPs using synchronous buck converters	February 2000	12
Powering Celeron-type microprocessors using TI's TPS5210 and TPS5211 controllers	February 2000	20
Simple design of an ultra-low-ripple DC/DC boost converter with TPS60100 charge pump	May 2000	11
Low-cost, minimum-size solution for powering future-generation Celeron™-type processors with peak currents up to 26 A	May 2000	14
Advantages of using PMOS-type low-dropout linear regulators in battery applications (PDF - 216 Kb)	August 2000	16
Optimal output filter design for microprocessor or DSP power supply (PDF - 748 Kb)	August 2000	22
Understanding the load-transient response of LDOs (PDF - 241 Kb)	November 2000	19

Title	Issue	Page
<b>Power Management (Continued)</b>		
Comparison of different power supplies for portable DSP solutions working from a single-cell battery (PDF - 136 Kb)	November 2000	24
Optimal design for an interleaved synchronous buck converter under high-slew-rate, load-current transient conditions (PDF - 206 Kb)	February 2001	15
-48-V/+48-V hot-swap applications (PDF - 189 Kb)	February 2001	20
Power supply solution for DDR bus termination	July 2001	9
Runtime power control for DSPs using the TPS62000 buck converter	July 2001	15
Power control design key to realizing InfiniBand <sup>SM</sup> benefits	First Quarter, 2002	10
Comparing magnetic and piezoelectric transformer approaches in CCFL applications	First Quarter, 2002	12
Why use a wall adapter for ac input power?	First Quarter, 2002	18
SWIFT <sup>TM</sup> Designer power supply design program	Second Quarter, 2002	15
Optimizing the switching frequency of ADSL power supplies	Second Quarter, 2002	23
Powering electronics from the USB port	Second Quarter, 2002	28
Using the UCC3580-1 controller for highly efficient 3.3-V/100-W isolated supply design	Fourth Quarter, 2002	8
Power conservation options with dynamic voltage scaling in portable DSP designs	Fourth Quarter, 2002	12
Understanding piezoelectric transformers in CCFL backlight applications	Fourth Quarter, 2002	18
<b>Interface (Data Transmission)</b>		
TIA/EIA-568A Category 5 cables in low-voltage differential signaling (LVDS)	August 1999	16
Keep an eye on the LVDS input levels	November 1999	17
Skew definition and jitter analysis	February 2000	29
LVDS receivers solve problems in non-LVDS applications	February 2000	33
LVDS: The ribbon cable connection	May 2000	19
Performance of LVDS with different cables (PDF - 57 Kb)	August 2000	30
A statistical survey of common-mode noise (PDF - 131 Kb)	November 2000	30
The Active Fail-Safe feature of the SN65LVDS32A (PDF - 104 Kb)	November 2000	35
The SN65LVDS33/34 as an ECL-to-LVTTL converter	July 2001	19
Power consumption of LVPECL and LVDS	First Quarter, 2002	23
<b>Amplifiers: Audio</b>		
Reducing the output filter of a Class-D amplifier	August 1999	19
Power supply decoupling and audio signal filtering for the Class-D audio power amplifier	August 1999	24
PCB layout for the TPA005D1x and TPA032D0x Class-D APAs	February 2000	39
An audio circuit collection, Part 1 (PDF - 93 Kb)	November 2000	39
1.6- to 3.6-volt BTL speaker driver reference design (PDF - 194 Kb)	February 2001	23
Notebook computer upgrade path for audio power amplifiers (PDF - 202 Kb)	February 2001	27
An audio circuit collection, Part 2 (PDF - 215 Kb)	February 2001	41
An audio circuit collection, Part 3	July 2001	34
Audio power amplifier measurements	July 2001	40
Audio power amplifier measurements, Part 2	First Quarter, 2002	26
<b>Amplifiers: Op Amps</b>		
Single-supply op amp design	November 1999	20
Reducing crosstalk of an op amp on a PCB	November 1999	23
Matching operational amplifier bandwidth with applications	February 2000	36
Sensor to ADC — analog interface design	May 2000	22
Using a decompensated op amp for improved performance	May 2000	26
Design of op amp sine wave oscillators (PDF - 56 Kb)	August 2000	33
Fully differential amplifiers (PDF - 51 Kb)	August 2000	38
The PCB is a component of op amp design (PDF - 64 Kb)	August 2000	42
Reducing PCB design costs: From schematic capture to PCB layout (PDF - 28 Kb)	August 2000	48

Title	Issue	Page
<b>Amplifiers: Op Amps (Continued)</b>		
Thermistor temperature transducer-to-ADC application (PDF - 97 Kb) .....	November 2000 .....	44
Analysis of fully differential amplifiers (PDF - 96 Kb) .....	November 2000 .....	48
Fully differential amplifiers applications: Line termination, driving high-speed ADCs, and differential transmission lines (PDF - 185 Kb) .....	February 2001 .....	32
Pressure transducer-to-ADC application (PDF - 185 Kb) .....	February 2001 .....	38
Frequency response errors in voltage feedback op amps (PDF - 184 Kb) .....	February 2001 .....	48
Designing for low distortion with high-speed op amps .....	July 2001 .....	25
Fully differential amplifier design in high-speed data acquisition systems .....	Second Quarter, 2002 ..	35
Worst-case design of op amp circuits .....	Second Quarter, 2002 ..	42
Using high-speed op amps for high-performance RF design, Part 1 .....	Second Quarter, 2002 ..	46
Using high-speed op amps for high-performance RF design, Part 2 .....	Third Quarter, 2002 ..	21
FilterPro™ low-pass design tool .....	Third Quarter, 2002 ..	24
Active output impedance for ADSL line drivers .....	Fourth Quarter, 2002 ..	24
<b>General Interest</b>		
Synthesis and characterization of nickel manganite from different carboxylate precursors for thermistor sensors (PDF - 194 Kb) .....	February 2001 .....	52
Analog design tools .....	Second Quarter, 2002 ..	50

## TI Worldwide Technical Support

### Internet

#### TI Semiconductor Product Information Center Home Page

support.ti.com

#### TI Semiconductor KnowledgeBase Home Page

support.ti.com/sc/knowledgebase

### Product Information Centers

#### Americas

Phone +1(972) 644-5580  
 Fax +1(972) 927-6377  
 Internet/Email support.ti.com/sc/pic/americas.htm

#### Europe, Middle East, and Africa

Phone  
 Belgium (English) +32 (0) 27 45 55 32  
 Finland (English) +358 (0) 9 25173948  
 France +33 (0) 1 30 70 11 64  
 Germany +49 (0) 8161 80 33 11  
 Israel (English) 1800 949 0107  
 Italy 800 79 11 37  
 Netherlands (English) +31 (0) 546 87 95 45  
 Spain +34 902 35 40 28  
 Sweden (English) +46 (0) 8587 555 22  
 United Kingdom +44 (0) 1604 66 33 99  
 Fax +(49) (0) 8161 80 2045  
 Email epic@ti.com  
 Internet support.ti.com/sc/pic/euro.htm

#### Japan

Fax International +81-3-3344-5317  
 Domestic 0120-81-0036  
 Internet/Email International support.ti.com/sc/pic/japan.htm  
 Domestic www.tij.co.jp/pic

#### Asia

Phone  
 International +886-2-23786800  
 Domestic Toll-Free Number  
 Australia 1-800-999-084  
 China 108-00-886-0015  
 Hong Kong 800-96-5941  
 Indonesia 001-803-8861-1006  
 Korea 080-551-2804  
 Malaysia 1-800-80-3973  
 New Zealand 0800-446-934  
 Philippines 1-800-765-7404  
 Singapore 800-886-1028  
 Taiwan 0800-006800  
 Thailand 001-800-886-0010  
 Fax 886-2-2378-6808  
 Email tiasia@ti.com  
 Internet support.ti.com/sc/pic/asia.htm

**Important Notice:** The products and services of Texas Instruments Incorporated and its subsidiaries described herein are sold subject to TI's standard terms and conditions of sale. Customers are advised to obtain the most current and complete information about TI products and services before placing orders. TI assumes no liability for applications assistance, customer's applications or product designs, software performance, or infringement of patents. The publication of information regarding any other company's products or services does not constitute TI's approval, warranty or endorsement thereof.

A070802